creative commons
COMMONS DEED

저작자표시-비영리-변경금지 2.0 대한민국

이용자는 아래의 조건을 따르는 경우에 한하여 자유롭게

- 이 저작물을 복제, 배포, 전송, 전시, 공연 및 방송할 수 있습니다.

다음과 같은 조건을 따라야 합니다:

저작자표시. 귀하는 원저작자를 표시하여야 합니다.

비영리. 귀하는 이 저작물을 영리 목적으로 이용할 수 없습니다.

변경금지. 귀하는 이 저작물을 개작, 변형 또는 가공할 수 없습니다.

- 귀하는, 이 저작물의 재이용이나 배포의 경우, 이 저작물에 적용된 이용허락조건을 명확하게 나타내어야 합니다.
- 저작권자로부터 별도의 허가를 받으면 이러한 조건들은 적용되지 않습니다.

저작권법에 따른 이용자의 권리는 위의 내용에 의하여 영향을 받지 않습니다.

이것은 이용허락규약(Legal Code)을 이해하기 쉽게 요약한 것입니다.

Disclaimer

dCollection

공학박사 학위논문

A study on filament breakup process of silicone oil/PMMA suspensions

Silicone oil/PMMA 현탁액의 필라멘트 끊김 공정에 관한 연구

2016 년 2 월

서울대학교 대학원

화학생물공학부

문 주 용

Abstract

A study on filament breakup process of silicone oil/PMMA suspensions

Joo Yong Moon
School of Chemical and Biological Engineering
The Graduate School
Seoul National University

The effect of particles dispersed in a Newtonian medium on the filament breakup of suspensions under extensional flow was investigated. In particular, the final stage of the breakup process was focused because the process in the final stage was more complicated and complex than in the initial stage. In order to study the effect of the particles, 10 μm poly(methyl methacrylate) (PMMA) particles with 0~20 wt% were dispersed in a silicone oil and the effects of the particles on the thinning dynamics and the shape of the filament were observed with time dependent changes in the minimum neck diameter (W: the shortest length of the filament).

The particles affected the dynamics of the thinning filament, and the role of the particles was different according to the stages of the breakup process. In the initial stage of the process, the particles decelerated the filament breakup process until the minimum thickness (W) of the filament became 5 D (D=10 μm: particle diameter), and then they accelerated the process rapidly until the pinch-off, which was the onset of filament rupture.

In order to investigate the effect of the particles on the thinning dynamics, the breakup velocity of 20 wt% PMMA suspension was compared with that of a silicone oil having the same viscosity and surface tension with the 20 wt% PMMA suspension. When W>35 D (350 μm), the time evolutions of minimum neck diameter for the PMMA suspension and the viscosity-matched silicone oil were almost the same. In this regime, the thinning dynamics of the two filaments was governed only by the bulk properties of the fluids. However, when the filament became thinner than 35 D, the thinning dynamics of the two fluids began to show differences even though they had the same properties. In addition to the increase in the effective viscosity, the particles decreased the breakup velocity more than the viscosity-matched silicone oil because the particles confined in the narrow filament channel disturbed the flow of the thinning filament under the extensional flow. In this way, the effect of the particles on the thinning filament could be confirmed while eliminating differences in the rheological properties of the two fluids.

The effect of the particles on the filament shape was investigated through the comparison of the filament shape between the 20 wt% PMMA suspension and the viscosity-matched silicone oil. When the filaments of the fluids were thicker than W=10 D (100 μm), the filament shape of the fluids was almost the same. It indicates the particles did not affect the shape of the filament in regime of W>10 D. The particles began to affect the filament shape when the filament became thinner than W=10 D. The filament surface of the PMMA suspension was rough and the shape of the filament became random for W<2 D, which led to a random pinch-off of the thinning filament. The randomness was induced because the local concentration of the particles confined in the filament became non-uniform as the

filament of the PMMA suspension was thin in the length scale of a particle diameter. The random distribution of the particles induced heterogeneity in the final stage of the filament thinning process, and the random distribution of the particles was quantified using the analysis of light intensity in the central part of the thinning filament.

Thus, the effect of the particles in the final stage of filament breakup was found to be more complicated than that in the initial stage, and we demonstrated that the particles dispersed in a Newtonian medium induced complex behaviors in the final stage of filament breakup. This work provides the information about the effect of the particles confined in the thinning filament on the dynamics and the shape of the filament for particulate suspensions. It is expected that the information about the role of the particles in the filament breakup process will be useful in designing the extensional process such as coating, jetting, spraying, among others.

Keywords: flow visualization, filament breakup, silicone oil/PMMA suspension, random pinch-off, random particle distribution

Student Number: 2008-22980

List of Contents

List of Figures

List of Tables

Chapter 1.

Introduction

1.1. General introduction

Understanding the extensional flow properties of particulate suspensions is important in many industrial processes such as inkjet printing, spraying, and coating, because complex behaviors are often observed during the extension, which leads to the formation of satellites (Wagner *et al*. 2005; Arnolds *et al*. 2010) as seen in Figure 1.1.1 and the acceleration of breakup (Furbank and Morris 2007; Bertrand *et al*. 2012; Bonnoit *et al*. 2012; van Deen *et al*. 2013), among others. These complex behaviors are induced through the use of different types of particles and polymers, and the effects of the added polymers have been reported in previous research.

Many researchers have studied the filament breakup process of the polymer solution depending on polymer concentration and molecular weight, among others (Zhang *et al*. 1996; Mun *et al*. 1998; Amarouchene *et al*. 2001; Anna and McKinley 2001; McKinley and Sridhar 2002; Stelter *et al*. 2002; McKinley 2005; Rodd *et al*. 2005; Tirtaatmadja *et al*. 2006; White *et al*. 2009; Sattler *et al*. 2012). The effect of polymers on the filament breakup under extensional flow has been primarily investigated using CaBER (Capillary Breakup Extensional Rheometer), and the elasticity of polymer solutions is known to delay the breakup in the final stage through forming cylindrical filaments and beads-on-a-string structures as seen in Figure 1.1.2 and 1.1.3 (Lee, M.-P *et al*. 1992; Li and Fontelos 2003; Oliveira and McKinley 2005; Clasen *et al*. 2006; Oliveira *et al*. 2006; Bhat *et al*. 2010, Sattler *et al*. 2012). In addition, the thinning dynamics of the polymer solution has been well described numerically (Keller and Miksis 1983; Entov and

Yarin 1984; James *et al*. 1987; Eggers 1993; Brenner *et al*. 1994; Renardy 1994; Petrie 1996; Entov and Hinch 1997; Chang and Demekhin 1999; Stokes *et al*. 2000; Rasmussen and Hassager 2001; Basaran 2002; Renardy 2002; Li and Fontelos 2003; Fontelos and Li 2004).

The effects of the particles on the filament breakup process began to be investigated by Furbank and Morris (2004). After that, much research (Bosse *et al*. 2005; Furbank and Morris 2007; Desse *et al*. 2009; Hameed and Morris 2009; Alexandrou *et al*. 2011; Bertrand *et al*. 2012; Bonnoit *et al*. 2012; van Deen *et al*. 2013; Zimoch *et al*. 2013, Saha *et al*. 2014; Dimic-Misic *et al*. 2015; Mathues *et al*. 2015; McCready and Burghardt 2015; Ogura *et al*. 2015; Ren *et al*. 2015; Zhao *et al*. 2015) have investigated the effect of the particles on the thinning filament under extensional flow, and they focused on the overall process of the drop formation from a macroscopic perspective. They discussed the dynamics of the thinning filament and the role of the particles on the breakup velocity of the filament.

In this way, much research had investigated the effect of the particles on the thinning filament under extensional flow macroscopically. However, the effect of the particles in the final stage of the breakup process is more complex than that in the initial and middle stages of the breakup process. Thus, it is important to observe the breakup process from the microscopic perspective, and it is necessary to observe the filament thinning process in the length scale of particle size.

Furthermore, the particles dispersed in a fluid can increase the non-uniformity of the suspensions by developing a number of structures, including particle aggregates (Ehrl *et al*. 2008; Gupta *et al*. 2011; Ozel *et al*. 2014), gels (van Vliet *et al*. 1991; So *et al*. 2004; Lu and Weitz 2013; Han and Kim 2015), and phase separations

(Linse and Lobaskin 1999; Fily and Marchetti 2012; Buttinoni *et al*. 2013), even in the quiescent state. Sometimes, the particles induce complex behaviors such as shear-thickening (Bender and Wagner 1996; Wagner and Brady 2009) or shear banding (Manneville 2008; Olmsted 2008) under the flow. The complexity introduced by these behaviors is one of the causes of the defects often observed in industrial processes. Therefore, the research on the heterogeneity and complexity due to the addition of the particles in the fluid is important both industrially and academically.

Under a flow field, the particles can increase the non-uniformity of the suspensions by forming particle alignment (Xue and Grest 1990; Won and Kim 2004), roller-like structure (DeGroot jr *et al*. 1994; Montesi *et al*. 2004; Vermant and Solomon 2005), network structure (Yanez *et al*. 1996; Wijmans and Dickinson 1998; van Opheusden and Molenaar 2014), and more. Most of these researches have been performed under shear flow. However, as the processes with a significant extensional flow, like coating and printing, come to the fore, the effect of the particles has also been studied under the extensional flow. We could observe that the particles induce the filament surface rough and the pinch-off process non-uniform. Therefore, it is necessary to learn more about the effect of the particles on the filament shape.

In this research, the effect of particles on the filament thinning behavior in the final stage of the breakup process was investigated. In the first step, we verified the effect of the viscosity of Newtonian fluids on the thinning dynamics of the filament without the particles and we compared this with that of the PMMA suspension. In addition, we made a comparison of the breakup process between the PMMA

suspension and the Newtonian fluid with the same viscosity and surface tension. Through the comparison, the effect of the particles on the filament breakup process could be observed, while maintaining the bulk effective fluid properties the same. Through this observation, we confirmed that the particles induce significant changes in the breakup velocity.

Furthermore, the particles induced a rough surface during the filament thinning. When the minimum neck diameter of the filament became thinner than two times the particle diameter, the particles induced random pinch-off: the filament shape became heterogeneous during the breakup process as the minimum neck diameter of the filament became thin in the length scale of the particle diameter. In the final stage of the filament breakup, the particles led to complex and random thinning dynamics because the dispersed particles were not uniformly distributed in the filament. Close to the pinch-off, the random distribution of the particles, having a 'finite-size effect', induced heterogeneity in the filament breakup process. We tried to analyze the non-uniformity quantitatively and clarify the cause of this heterogeneity, which appeared in the final stage of the filament breakup of the silicone oil/PMMA suspension. In this way, we investigated the effect of the particles on the filament breakup, while focusing on the final stage of the breakup process.

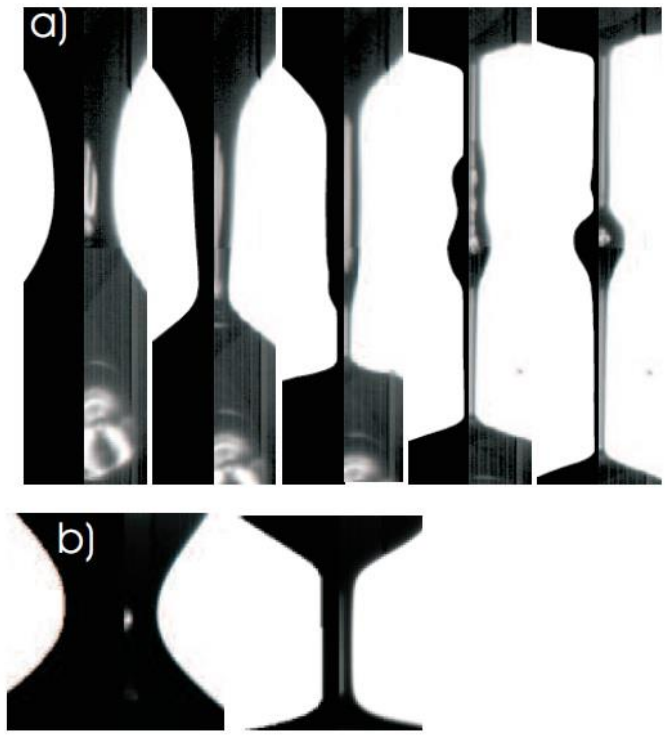

Figure 1.1.1. The droplet detachment process of an aqueous 100 ppm PEO solution at different time steps $t_c - t$ relative to the time t_c at which the filament is formed. The left half of the pictures is plots from numerical simulations, the right half are experimental photographs. (a) nozzle radius R=1.5 mm (pictures are 1.2×9 mm) $t_c - t$=6, 2, 0, -3, -5 ms, (b) R=0.4 mm (pictures are 0.9×0.9 mm) $t_c - t$=1, 0 ms. The model parameters used for the numerical simulation were $\eta_P = 3.7 \times 10^{-4}$ Pa s for the polymeric contribution to the viscosity, a polymer timescale of $\lambda = 1.2 \times 10^{-2}$, and an elasticity parameter of $b = 2.5 \times 10^4$. The solvent viscosity (water) is $\eta_S = 1 \times 10^{-3}$ Pa s and the surface tension is $\gamma = 6 \times 10^{-2}$ N/m. (Wagner *et al*. 2005).

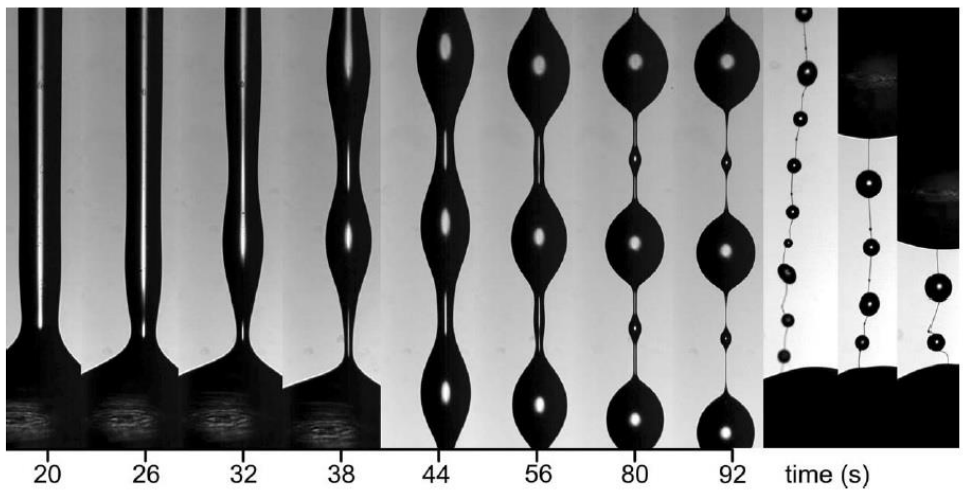

Figure 1.1.2. The final stages of the break-up of a droplet of human saliva (for $t \leq 92$ s images are 0.21×1.37 mm, the last three images are 0.42×3.1 mm). Time is counted from the formation of a cylindrical filament, which is shown in the first panel. The filament remained stable for several minutes, and final rupture was initiated by agitating the system. This is shown in the magnified last three images on the right. They illustrate the stiffness of the (solid) polymeric fiber that is formed between the remaining droplets and which remains essentially straight. (Sattler *et al*. 2012).

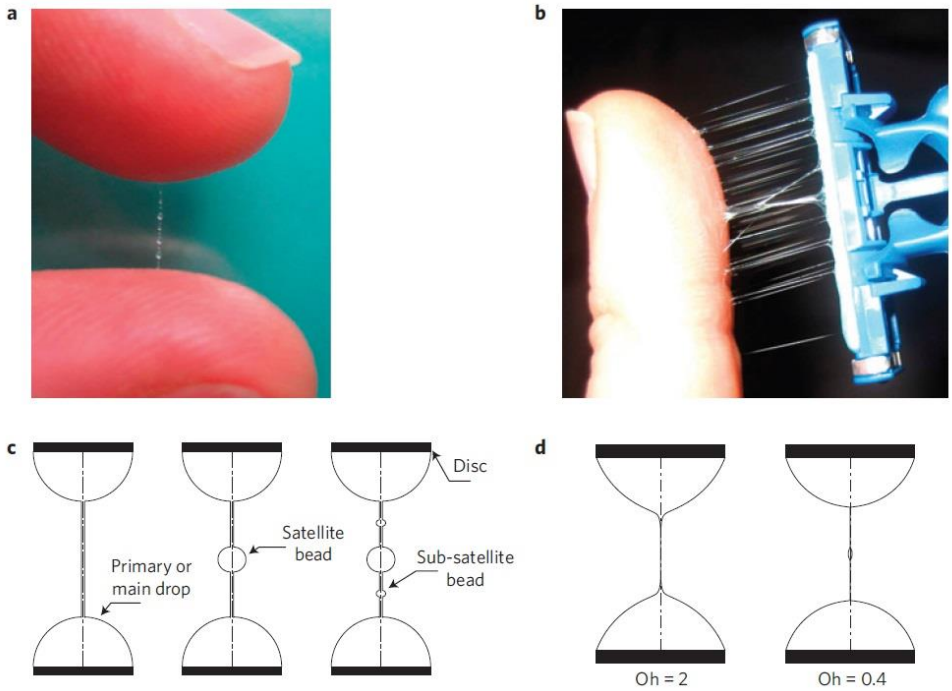

Figure 1.1.3. Using a 'digital rheometer' to measure the stringiness or pituity of various complex liquids, and filament morphologies near pinch-off. (a) A drop of sublingual saliva placed between a thumb and forefinger and elongated to form a BOAS (Beads-on-a-string) morphology. (b) A film of water-soluble polymer elongated from the lubricating strip on a disposable razor. The enhanced viscosity and elasticity of the synthetic polymer solution in results in a slippery and lubricious film but inhibits the formation of beads. (c) Sketches of viscoelastic filaments exhibiting different BOAS morphologies reported in the literature. (d) Computed interface shapes of pinching Newtonian liquid bridges with aspect ratio Λ =3. Left: break-up of a high-viscosity filament (Oh=2), and right: break-up of a low-viscosity filament (Oh=0.4). The dash–dot line in (c), (d) is the axis of symmetry. (Bhat *et al*. 2010).

1.2. Outline of the thesis

The thesis consists of background, experimental methods, results and discussion, and summary chapters. Each chapter includes the following contents.

Chapter 2 summarizes the background of the previous research of filament breakup process, which is divided into start of study on filament breakup process and previous study on filament breakup of simple fluids and that of suspensions. The first part of Chapter 2 summarizes the first study on filament breakup and its disadvantages and limitations and the second part describes the thinning dynamics of the Newtonian fluids through a governing equation of the thinning filament. The governing equation is defined by viscosity and surface tension of the fluids. The last part of Chapter 2 summarizes the previous studies on filament breakup process of suspensions and their limitation.

Chapter 3 describes experimental methods used in this research. The first and second parts of Chapter 3 explain information of materials, sample preparation methods, and experimental setup in order to observe the final stage of the filament breakup process. The last part describes characterization methods for thinning filament, which are divided into measurement of minimum neck diameter (W), measurement of thickness difference with the filament height (ΔX_i), measurement of roughness of filament surface, analysis of light intensity in the central part of the filament.

Chapter 4 describes the results and discussion about the effect of the particles added in Newtonian fluid on the filament breakup process. Before observing the effect of the particles, the thinning dynamics of pure Newtonian fluids is discussed

in the first part. The second and third parts of Chapter 4 describe the effect of the particles on the thinning dynamics of suspensions and the filament shape using the characterization method explained in Chapter 3. The particles induced non-uniform breakup process of the suspensions in the final stage of the process, the cause of the heterogeneity is discussed in the last part of Chapter 4.

Chapter 5 summarizes the results on the works about the effect of the particles confined in thinning filament on the filament breakup process of particulate suspensions.

Chapter 2.

Background

2.1. Start of study on filament breakup process

The filament breakup process under extensional flow is driven by capillary force of the thinning filament. Therefore, it is so-called capillary-driven flow. The filament breakup process can be observed during jetting, dripping faucet, and bridging liquid between two disks. The processes have been studied in much research for a long time because the extensional flow is significant in many processes, such as coating, spraying, and printing. The filament breakup process has been studied since the end of the 19th century by Plateau (1843, 1849) and Rayleigh (1892).

Firstly, Plateau (1843, 1849) observed the stability of the thinning filament in liquid bridge process between two disks. However the studies of Plateau had a critical disadvantage. They used ‘Plateau tank’ as an experimental setup. The thinning fluids and the two disks were set up within the ‘Plateau tank’ and the tank was filled additional fluid. It indicates that filament became thin within circumferential outer fluid as seen in Figure 2.1.1 (Spiegelberg 1994). The important thing in this figure is that the breakup process happened for approximately 3 hours. It is why Plateau used this tank to observe that the additional fluid filled within the tank decelerated the filament breakup process because the filament breakup process was too fast to be observed and investigated.

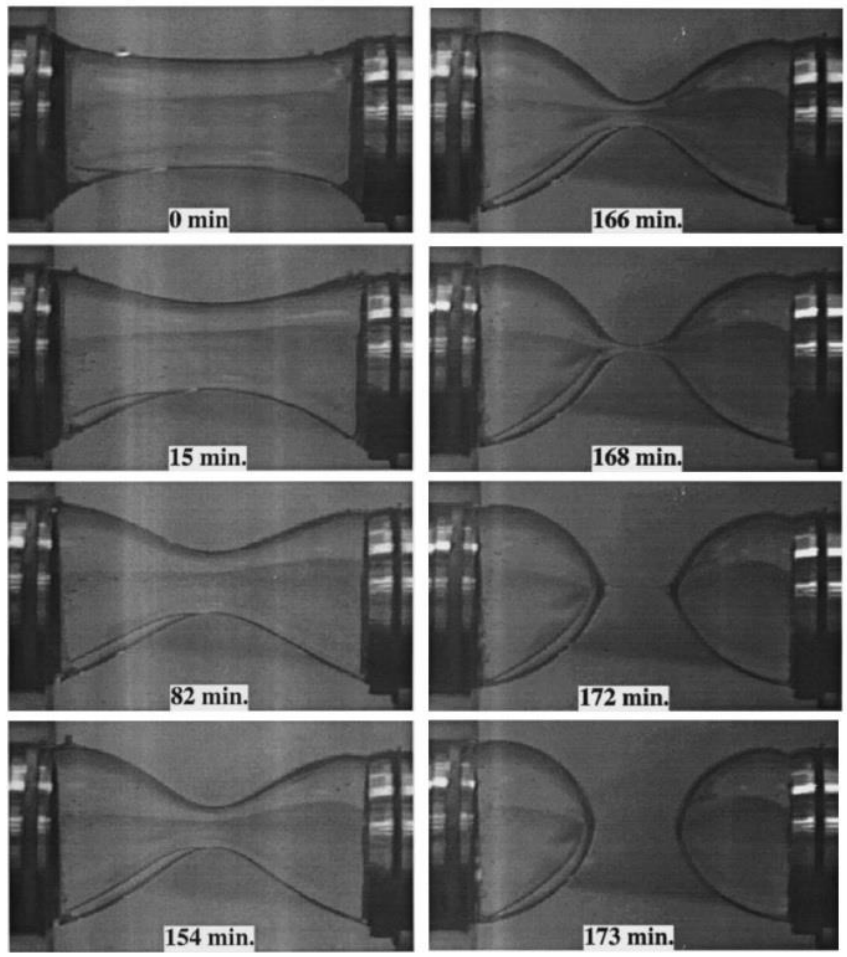

Figure 2.1.1. Liquid-bridge evolution starting from an unstable configuration. The disk diameter was 3.8 cm, the Reynolds number was 3.731023. The outer fluid, which eliminated buoyancy forces, had a viscosity approximately 1000 times smaller than the inner fluid. (Spiegelberg *et al*. 1994).

After the studies of Plateau, Rayleigh (1892) investigated the initial stage of drop formation process and observed that the filament of simple fluids was shrunk exponentially in the initial regime. However, Rayleigh could not observe the final stage of the breakup or pinch-off process due to limitation of the camera performance. Because the final stage of the process happened for less than 1 second in μm length scale. The reason that he could not investigate the final stage of the process was the same why Plateau used the ‘Plateau tank’. In this way, Rayleigh (1892) reported the thinning dynamics of filament under extensional flow for the first time.

2.2. Previous study on thinning dynamics of simple fluids

Nowadays, the filament breakup process including the final stage has been investigated for the development of optics. There is much research, which observed the thinning filament of simple fluids such as Newtonian fluids and polymeric solutions using a high-speed camera. Through the research, the thinning dynamics of the simple fluids has been well understood theoretically. A number of experimental and theoretical researches for the filament breakup of the fluids were reviewed by Eggers (1997). In this Section, the thinning dynamics of the fluids will be summarized briefly.

The dynamics of the thinning filament was well described by Rothert *et al*. (2003) as three successive flow regimes, which consist of an accelerated flow regime, a Stokes flow regime, and a Navier-Stokes flow regime. The first accelerated flow regime was discussed by Rayleigh (1892) firstly. When the filament begins to be thinned from the static state, the neck radius of the thinning filament decreases exponentially with processing time. The behavior of the accelerated flow is depicted as seen in Figure 2.2.1 (Rothert *et al*. 2003). The change of the neck radius is fitted well with exponential curves.

The accelerated flow regime is followed by the Stokes flow regime. The breakup velocity is described by the capillary, inertia, and viscous forces. The capillary force induced by surface tension of medium is the driving force for the filament breakup, while the inertia and viscous forces play a role as a resistance to the driving force. However, in the Stokes regime, the inertia force can be neglected. The important feature in the Stokes regime is that the breakup velocity is almost

the constant, in other words, the minimum neck diameter (=neck radius $\times 2$) decreases linearly with time. The linear decrease can be confirmed in Figure 2.2.1 for $t\text{-}t_0$>-10 ms. In case of Newtonian fluids having low viscosity, the inertia force can be neglected until pinch-off state. The breakup velocity of the fluids can be expected through the simple equation by Eggers (1993) as defined in Equation (2.2.1).

$$W = 0.0608 \times \frac{\gamma}{\eta}(t - t_p). \tag{2.2.1}$$

W : Minimum neck diameter [μm]

γ : Surface tension [mN/m]

η : Viscosity [Pa s]

$t - t_p$: Processing time - pinch-off time [ms]

This thinning equation can be applied to fluids of moderate *Ohnesorge* number as defined in Equation (2.2.2).

$$Oh = \frac{\eta}{\sqrt{\rho \gamma R}}. \tag{2.2.2}$$

η : Viscosity [Pa s]

ρ : Density of fluid [kg/m^3]

γ : Surface tension [mN/m]

R : Jet radius [mm]

And Papageorgiou (1995) determined the governing equation of the minimum neck diameter for Newtonian fluids, which have high viscosity and large *Ohnesorge* number but the inertia can be still neglected, as defined in Equation (2.2.3).

$$W = 0.1418 \times \frac{\gamma}{\eta}(t - t_p)\,. \tag{2.2.3}$$

W : Minimum neck diameter [μm]

γ : Surface tension [mN/m]

η : Viscosity [Pa s]

$t - t_p$: Processing time - pinch-off time [ms]

The inertia force is induced by the stagnation point of the filament which is the central part of the filament without a velocity from the start of the breakup process. However, when the highly viscous fluids are thinned, the inertia force can no longer be neglected as approaching the pinch-off state because of the stagnation point of the highly viscous fluid. In this case, the breakup process enters the Navier-Stokes regime in the final stage of the process. As explained before, the inertia force is a resistance to the capillary force. Therefore, increase of the inertia force decelerates the breakup velocity and the curve of the minimum neck diameter with time for the fluids having high viscosity is convex downward slightly as shown in Figure 2.2.2 (Rothert *et al*. 2003). The thinning law of the inertia-dominated fluids was described by Day *et al*. (1998) as defined in Equation (2.2.4).

$$W = 1.28 \times \left(\frac{\gamma}{\eta} \right)^{1/3} (t - t_p)^{2/3} . \qquad (2.2.4)$$

W : Minimum neck diameter [μm]

γ : Surface tension [mN/m]

η : Viscosity [Pa s]

$t - t_p$: Processing time - pinch-off time [ms]

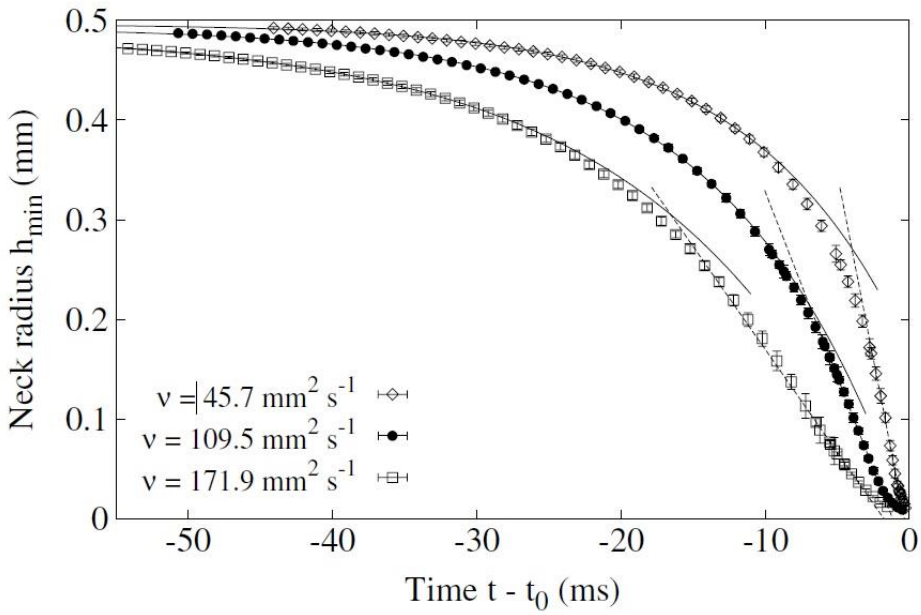

Figure 2.2.1. Time evolution of the neck radius for three different viscosities. The solid curves are exponential fits whereas the dashed lines are linear fits according to Stokes flow. (Rothert *et al*. 2003).

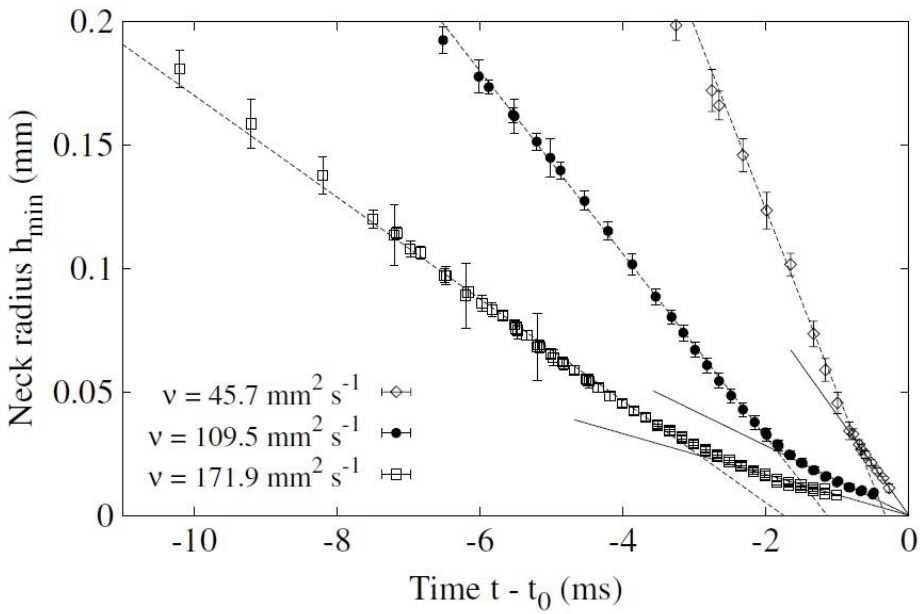

Figure 2.2.2. Time evolution of the neck radius in the last stage of the pinch-off. The dashed lines are linear fits according to Stokes flow and the solid ones describe the linear behavior in the Navier-Stokes regime. (Rothert *et al*. 2003).

2.3. Previous study on filament breakup of suspensions

The thinning dynamics of particulate suspensions has not been understood perfectly. However, some researchers had tried to describe the effect of the particles confined in the thinning filament on breakup velocity of the suspensions. The effect of particles was investigated firstly by Furbank and Morris (2004): they visualized and analyzed the drop formation process of suspensions using a high-speed camera as shown in Figure 2.3.1. (a) and (b). They observed pinch-off structures of the thinning filament and compared with that of the pure liquid. When the particle concentration was low ($\phi \leq 0.10$), the pinch-off structures were similar to that of the Newtonian fluid. However, the particles could be confined in the thinning filament and the particles sometimes led to the formation of satellite. In case of suspensions of high particle concentration ($0.15 \leq \phi \leq 0.40$), the pinch-off structures seemed as thick cone-like structures. In addition, they described the effect of the particles on pinch-off structure like this, 'Particles are found to substantially suppress the number of satellite drops at higher ϕ' and the particles made lager satellite compared with Newtonian fluids.

Later, Furbank and Morris (2007) reported the thinning dynamics of the suspensions during drop formation process. They observed the temporal evolution of the minimum neck diameter (W) with various particle concentrations and the viscosity of the suspending medium using poly (methyl methacrylate) (PMMA) particles having diameters of 106~125 and 212~250 μm and a suspending medium of polyalkylene glycol solution. They described the filament breakup process using two flow regimes. The particles reduced the breakup velocity in the first regime

due to the increase of the effective viscosity of suspensions induced by the addition of the particles. The regime was termed ‘effective regime’. After the effective regime, the particles began to accelerate the breakup process in the second regime as approaching pinch-off state. However, they did not clearly explain the precise boundary between the two flow regimes. Furthermore, they observed that the particles induced some fluctuation in the breakup velocity for the suspensions as seen in Figure 2.3.2. However, they did not discuss the cause of the non-uniformity.

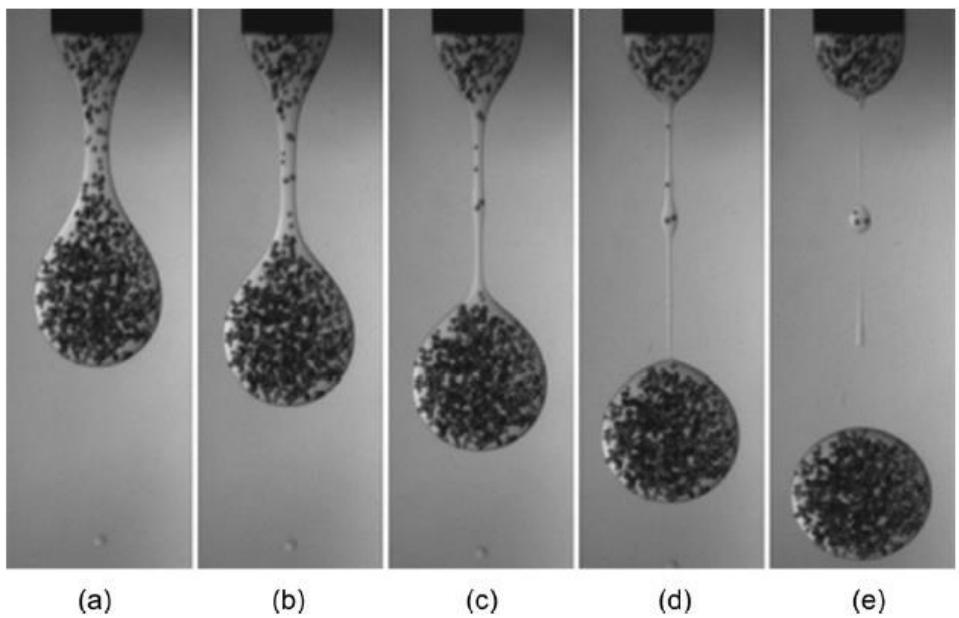

Figure 2.3.1. (a) Evolution of the suspension thread up to and slightly beyond pinch-off for ϕ=0.05, d=0.32 cm, d_p =212–250 μm into silicone oil with Q=1.8 cm^3/min (Re=0.04). The time between frames is 1/30 s. (Furbank and Morris 2004).

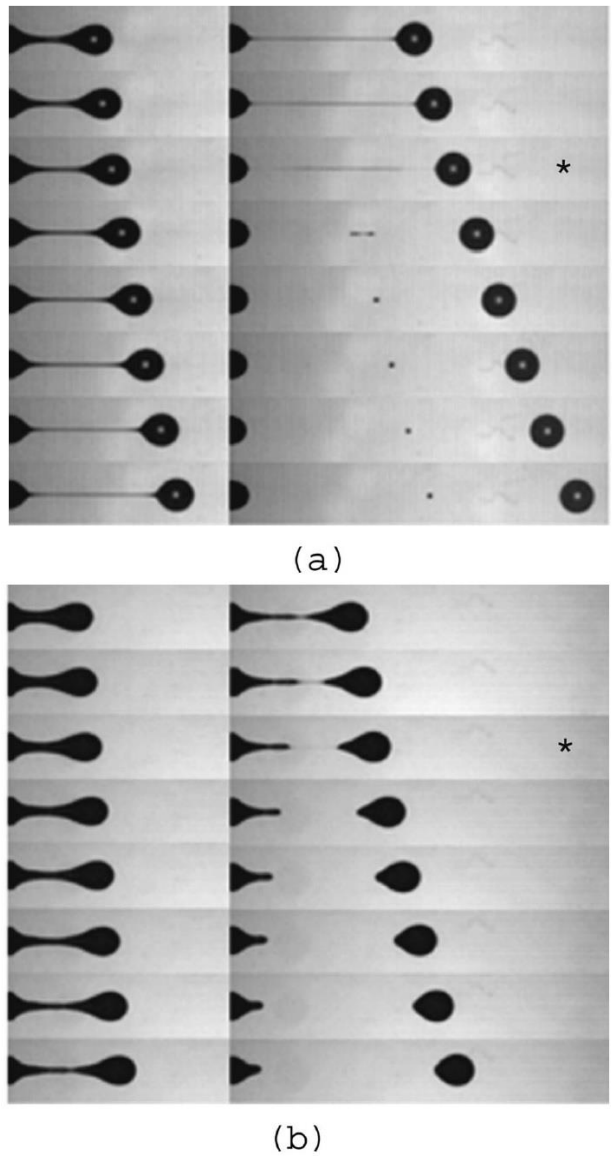

Figure 2.3.1. (b) Evolution of the liquid/suspension thread during necking through pinching for pure liquid (a) and suspension (ϕ=0.20) (b) into ambient air for d=0.32 cm, d_p=212–250 μm, Q=0.5 cm^3/min (Re=0.01). The time between frames is 1/250 s. Gravitational acceleration is to the right. (ϕ: particle concentration, d: outer diameter of a tube, d_p: particle diameter, Q: flow rate). (Furbank and Morris 2004).

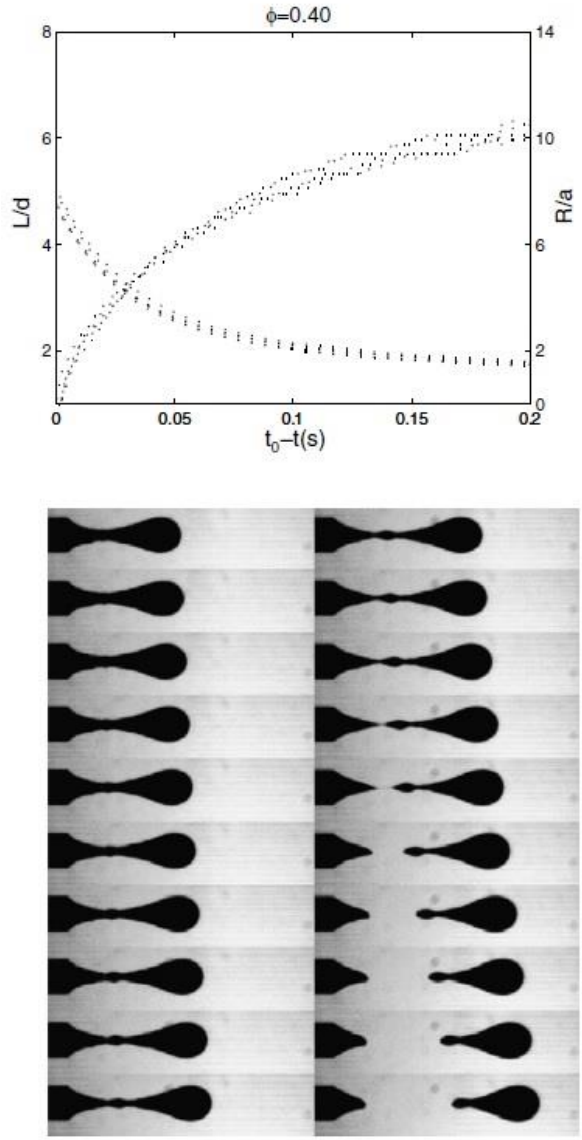

Figure 2.3.2. L/d and R/a measurement for ϕ =0.40 with the corresponding photographic sequences, for d=0.32 cm, d_p=212–250 μm. The time between images is 1/500 s. (ϕ: particle concentration, d: outer diameter of a tube, d_p: particle diameter. L: length of droplet). (Furbank and Morris 2007).

Since the works of Furbank and Morris (2004, 2007), Bonnoit *et al*. (2012) argued that there is another flow regime in the filament breakup process. They classified the breakup process of the filament as three regimes, which consist of the effective, the interstitial, and the acceleration regime. In the initial stage of the process, the effective viscosity of suspension governed the breakup velocity; thus, it was the 'effective regime' as reported in Furbank and Morris (2007). The final stage was the acceleration regime, in which the particles increased the breakup velocity while approaching the pinch-off. Different to Furbank and Morris (2007), there existed an interstitial regime, in which the thinning dynamics was determined only by the properties of the suspending medium, not the properties of the suspensions, in the middle stage of the breakup process. The crossover point between initial stage and interstitial stage varied about W=5~8 D with a particle size and a particle concentration. In this regime, the curves for the time evolution of the minimum neck diameter appeared to collapse onto a single curve regardless of the particle concentration as depicted in Figure 2.3.3. This indicates that a regime exists where the particles do not have any influence on the breakup velocity of the thinning filament in the middle stage of the breakup process. However, the convergence of the curves of the minimum neck diameter is necessary to be observed in length scale of μm because Bonnoit *et al*. observed the thinning filament macroscopically.

After the work of Bonnoit *et al*. (2012), much research has discussed the dynamics of the thinning filament for suspensions. Bertrand *et al*. (2012) studied the effect of the volume fraction of the particles on the drop formation and the shape of the filament. They described the thinning dynamics of suspensions using

three successive flow regimes of Bonnoit *et al*. (2012). They tried to investigate the effect of the particles on free surface of the filament. However, the effect of the particles was described only about the length of the thinning filament at pinch-off state and rough surface of the filament observed macroscopically as seen in Figure 2.3.4. van Deen *et al*. (2013) investigated the influence of the individual particles confined in the thinning filament on the thinning dynamics using particulate suspensions of small volume fractions (ϕ <6 %). They showed that even a single particle could modify the thinning dynamics of the filament strongly through the images as seen in Figure 2.3.5. McIlroy and Harlen (2014) studied the thinning dynamics of the suspensions numerically by constructing a simple one-dimensional model. They explained the three flow regimes of the filament theoretically.

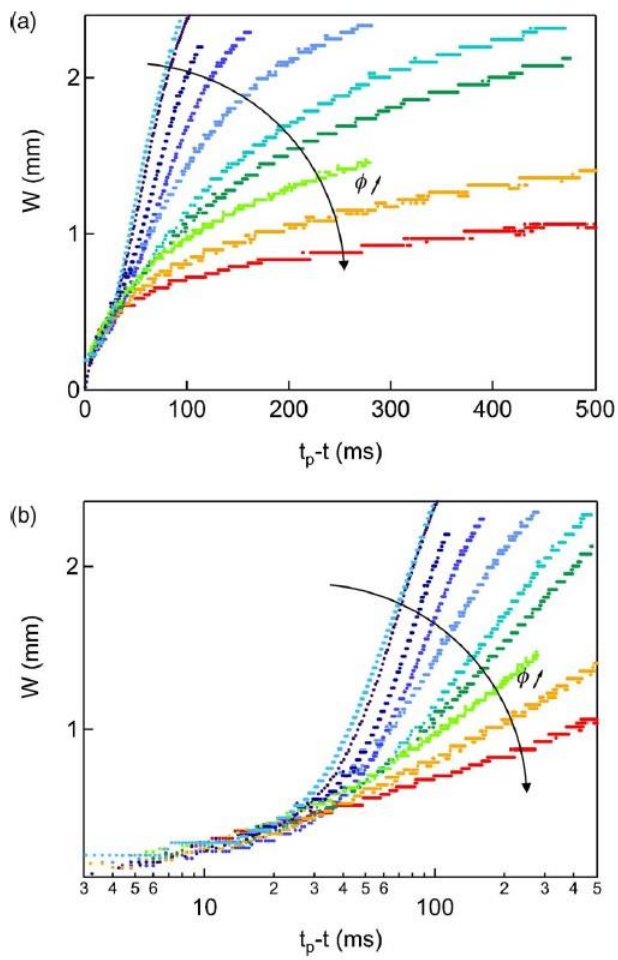

Figure 2.3.3. Time evolution of the minimum neck diameter W for suspensions with volume fractions ϕ =15, 20, 30, 40, 45, 48, 50, 53, 55 % with grain diameter d=40 μm. The leftmost curve (cyan online) corresponds to the pure interstitial fluid (ϕ =0). The origin of the x-axis is given by the time of the pinch for each suspension; the curve for the interstitial fluid is shifted by Δt_{SE} =−20 ms. (a) lin-lin representation (b) lin-log representation allowing for a better visibility of the short times close to pinch off. (Bonnoit *et al*. 2012).

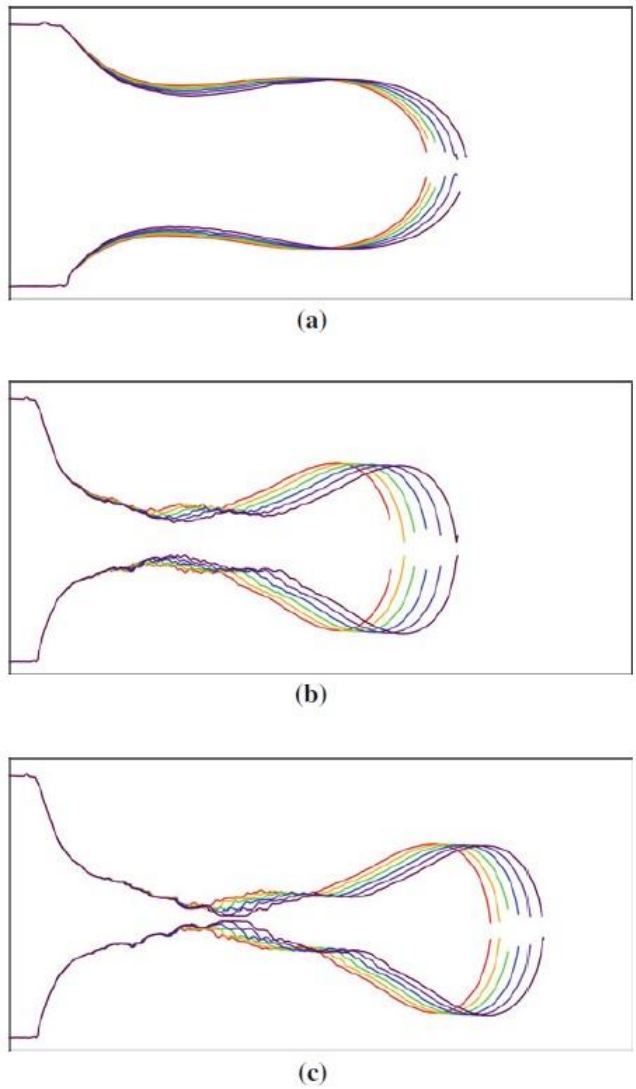

Figure 2.3.4. Drop shape in the different detachment regimes for a suspension of particle of diameter d=140 μm and volume fraction ϕ =40 %. (a) Effective fluid regime. Time step between two successive profiles Δt =25 ms, aspect ratio 1:1.01. (b) Interstitial oil regime. Time step between two successive profiles Δt =2.5 ms, aspect ratio 1:1.89. (c) Final detachment regime. Time step between two successive profiles Δt =1.25 ms, aspect ratio 1:1.89. (Bertrand *et al*. 2012).

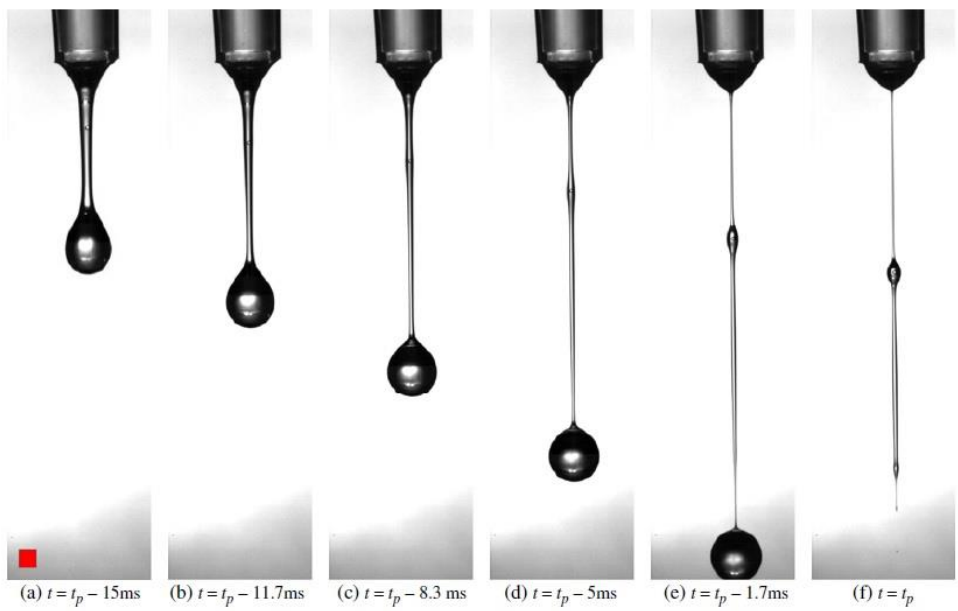

Figure 2.3.5. Example of the effect of a particle on the droplet detachment. For illustrative reasons, pictures using a large particle (d_{part}=250 μm) have been used. The *box* in the *bottom left* is 1 mm×1 mm. (van Deen *et al*. 2013).

In this way, the addition of the particles in the Newtonian fluids causes non-uniform and complex filament breakup process compared with that of Newtonian fluids. There is much research on the filament thinning of the suspensions (Bosse *et al*. 2005; Desse *et al*. 2009; Hameed and Morris 2009; Alexandrou *et al*. 2011; Zimoch *et al*. 2013, Saha *et al*. 2014; Dimic-Misic *et al*. 2015; Mathues *et al*. 2015; McCready and Burghardt 2015; Ogura *et al*. 2015; Ren *et al*. 2015; Zhao *et al*. 2015). They investigated how the particles affect the filament breakup process macroscopically. However, it is necessary to be observed in length scale of μm because the complex nonlinear behaviors of suspensions under extensional flow happen in the vicinity of the point where the filament breaks up.

Chapter 3.

Experimental methods

3.1. Sample preparation

Materials

A silicone oil/PMMA suspension was used as a model system. Spherical mono-dispersed poly(methyl methacrylate) (PMMA) particles were dispersed in a silicone oil, which is a Newtonian fluid. Two as-supplied silicone oils (Shinetsu, Inc., Japan) were used with different viscosities, η =0.01 Pa s (denoted as *SO-0.01*) and 10 Pa s (*SO-10*) at 20 ℃, but almost the same surface tension and density, $\gamma = 21 \pm 0.5$ mN/m and ρ =1,070 kg/m^3. The PMMA particles had a diameter of approximately 10 μm and a density of 1,180 kg/m^3. The density was well matched with the silicone oil, and the particle sedimentation could be neglected during the experiments.

Preparation method

The two silicone oils (*SO-0.01* and *SO-10*) were mixed at different ratios in order to control the viscosity of the suspending medium without critical changes in the other properties because the two silicone oils having different viscosities of 0.01 Pa s and 10 Pa s, but almost same surface tension and density. The thinning dynamics of the Newtonian fluid is governed by the viscosity and surface tension of the medium. The medium viscosity was varied only in this research. The PMMA particles were suspended in a silicone oil with a viscosity of 0.40 Pa s (*SO-0.40*) formed through mixing the two silicone oils (*SO-0.01* and *SO-10*) at a ratio of 3:2 (wt%). The PMMA particles added in *SO-0.40*, then mixed using magnetic stirrer

for 1 hr. The suspension was well dispersed because both the silicone oil and PMMA particles are hydrophobic. The particle concentration was ϕ=0~20 wt% and the effective viscosity (η_{eff}) of the PMMA suspensions is presented in Figure 3.1.1. The viscosity was measured using ARES (Advanced Rheometrics Expansion System; TA Instruments, Inc., USA) with a 50 mm parallel plate at 25 ℃. The effective viscosity of the PMMA suspension at ϕ=20 wt% was increased to approximately 0.71 Pa s. The measured viscosity of the PMMA suspension was compared with the Krieger-Dougherty equation as defined in Equation (3.1.1) (Krieger and Dougherty 1959). The viscosity of the suspending medium (η) was 0.40 Pa s, ϕ_{vol} was the particle volume fraction, and the maximum packing volume fraction was ϕ_{max}=0.64. The measured effective viscosity aligned well with the calculated ones.

$$\eta_{eff}\left(\phi_{vol}\right) = \eta\left(1 - \frac{\phi_{vol}}{\phi_{\max}}\right)^{-1.82} . \qquad (3.1.1)$$

In order to investigate the effect of the added particles on the filament breakup process, a 20 wt% PMMA suspension and a viscosity-matched silicone oil having almost the same viscosity and surface tension, 0.71 Pa s and 20.5 mN/m with the 20 wt% PMMA suspension were prepared. The viscosity-matched silicone oil was made by mixing *SO-0.01* and *SO-10* at a ratio of 54:46 (wt%). By comparing the thinning behavior of the two fluids, the effect of the particles on a thinning filament under extensional flow could be investigated with nearly identical viscosity and

surface tension, which govern the thinning dynamics of Newtonian fluids.

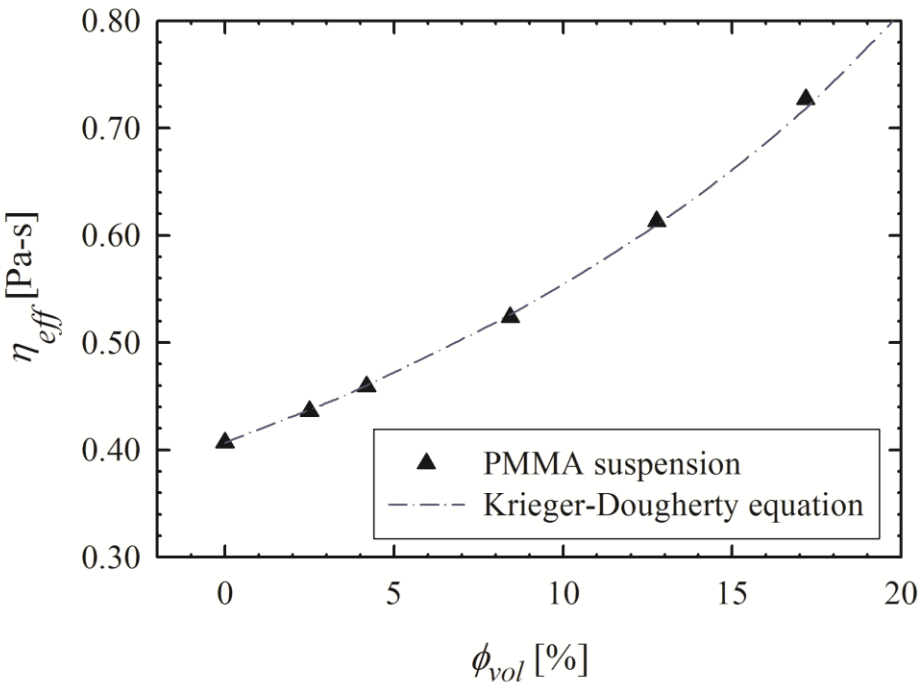

Figure 3.1.1. Effective viscosity of the silicone oil/PMMA suspension (symbol) and calculated viscosity of suspension using Krieger-Dougherty equation (dash with line) as a function of the particle volume fraction.

3.2. Experimental setup

3.2.1. Modification of UTM

A universal testing machine (UTM; LF Plus, Lloyd Instruments, Inc., UK) was modified in order to induce an extensional flow. Both clip parts of the UTM were modified as depicted in Figure 3.2.1, with two circular parallel plates with a diameter of 3 mm. The sample was loaded between the two plates, and the upper plate was moved upward in order to induce an extensional flow. The moving speed of the upper plate was 1 mm/s and the gap between the two plates was 1.5 mm, which was half of the plate diameter. The half of the plate diameter is suitable value for the gap between the two plates in order to induce stable extensional flow. The modified UTM had advantages compared with CaBER (Capillary Breakup Extensional Rheometer) used in the research about liquid bridge or filament breakup process. It was easy to control extension rate even it was slow under the extension rate of $\dot{\varepsilon} = 1\ s^{-1}$ and had wide empty space for visualization setup, a high-speed camera and a light source.

Figure 3.2.1. Modified section of the UTM. The diameters of the plates were 2, 3, and 5mm.

3.2.2. Visualization setup

The high-speed camera (Photron Fastcam Ultima 512, Photron, Inc., USA) was used. It took 4,000 frames per second (fps) at a resolution of 256×512 pixels. The high-speed camera with a ten-fold objective lens and a twelve-fold adapter was set up on the modified UTM as depicted in Figure 3.2.2. (a) in order to observe the motion of the 10 μm PMMA particles in the final stage of the filament breakup process. In this process, 1 pixel of the image represented an area of 1.94 μm×1.94 μm. The images with a resolution of 256×512 pixels covered an area of 486.4 μm×972.8 μm. The observing area was fixed during process as seen in Figure 3.2.2. (b). 250 W halogen light (BMH-250, Mejiro precision, Japan) was used for backlight illumination. Using this visualization setup, the final stage of the filament breakup process could be observed in the μm-length scale for tens and hundreds of milliseconds.

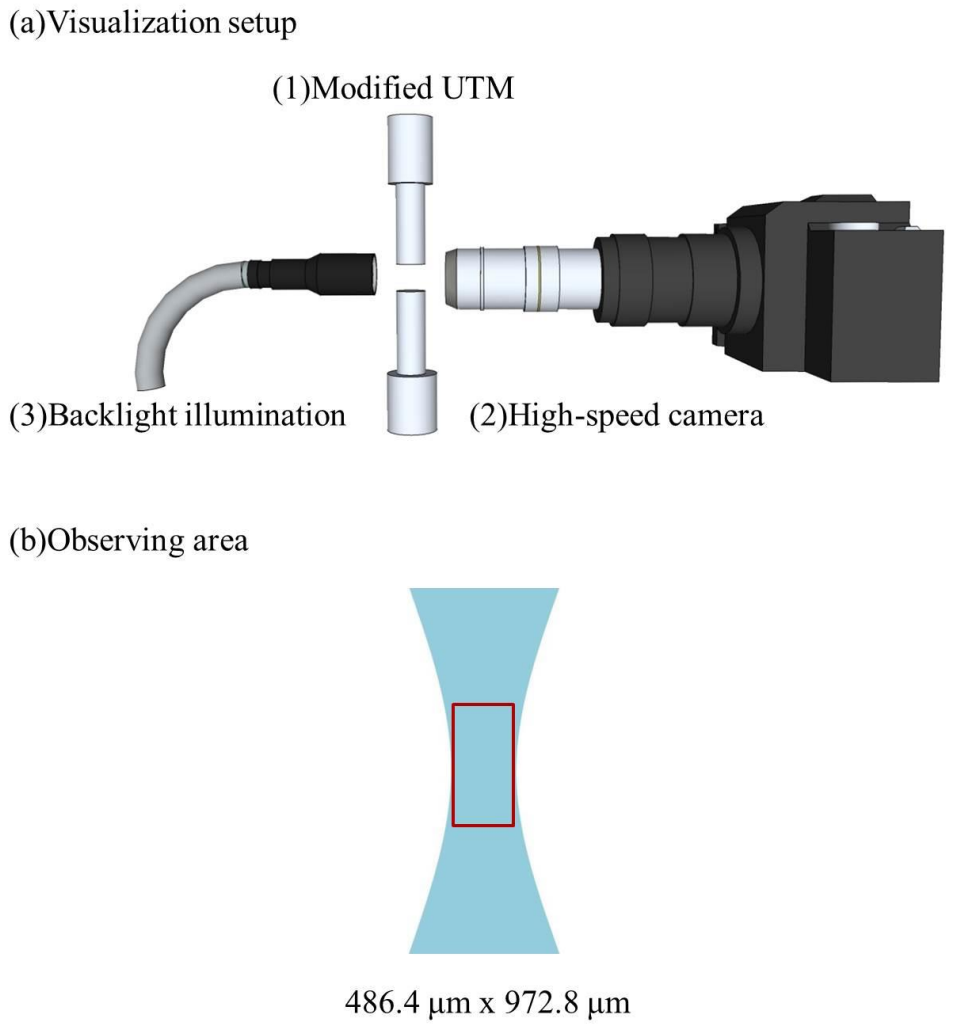

Figure 3.2.2. (a) Schematic of the modified UTM and visualization setup and (b) observing area.

3.3. Characterization of thinning filament

3.3.1. Measurement of minimum neck diameter (*W*)

In the research about the filament breakup process under extensional flow, the time evolution of the minimum neck diameter (*W*), which is the minimum diameter of the thinning filament as depicted in Figure 3.3.1, is a matter of primary concern. Because the dynamics of the thinning filament can be confirmed using the minimum neck diameter. In order to obtain the minimum neck diameter, the coordinates of the free surface of the thinning filament were extracted from the recorded images by MATLAB. MATLAB code found the thinnest part of the filament, and the length of the thinnest part was obtained. From the obtained minimum neck diameter, the time evolution of that could be observed with processing time. Example of the change of the minimum neck diameter as a function of time is shown in Figure 3.3.1. In this graph, the abscissa represents t_p–t [ms], t_p is the pinch-off time [ms] (i.e. the time of the complete filament breakup), and t is the processing time [ms]. The process direction is toward the left side of the graph, and the filament finally breaks up at t_p–t=0. The ordinate represents the minimum neck diameter, and the slope in this graph is the breakup velocity of the thinning filament (*V*) [mm/s] as defined in Equation (3.3.1):

$$V = \frac{dW(t)}{dt}. \tag{3.3.1}$$

The extension rate was calculated from the minimum neck diameter *W(t)* of the thinning filament using Equation (3.3.2), as follows:

$$\dot{\varepsilon} = -\frac{2}{W(t)}\frac{dW(t)}{dt}. \qquad (3.3.2)$$

In this thesis, the calculated extension rate was $\dot{\varepsilon}$ =0.001~1 s^{-1}. The extension rate was induced slowly in order to visualize very fast process of filament breakup in final stage.

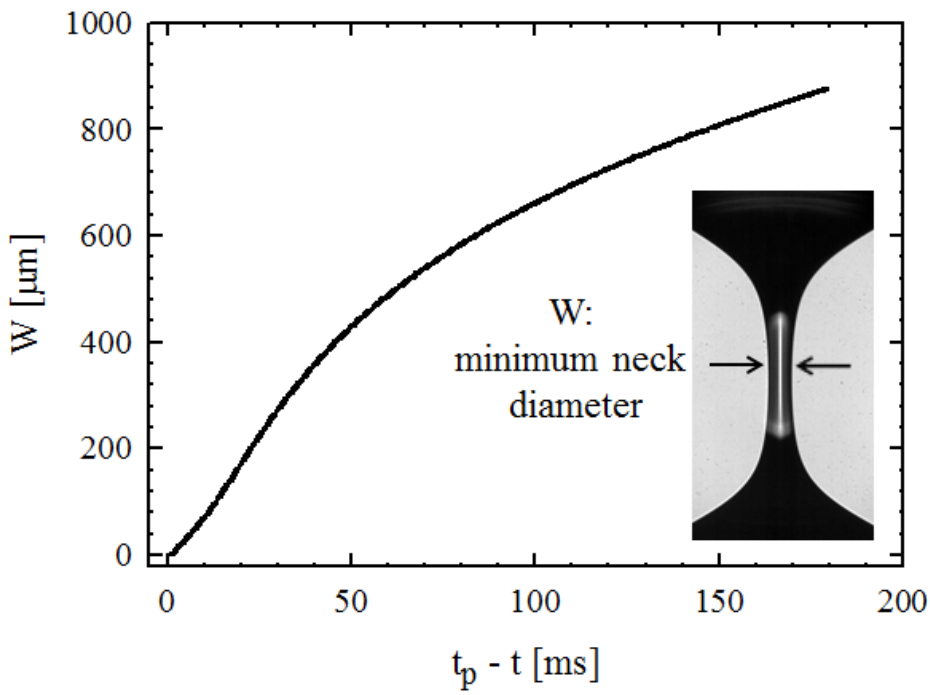

Figure 3.3.1. Time evolution of the minimum neck diameter (*W*) during the filament breakup (t_p: pinch-off time [ms], t: processing time [ms]). The direction of the process is toward the left side of the graph, and the filament finally breaks up at t_p–t=0.

3.3.2. Measurement of thickness difference (ΔX_i)

In order to quantify the influence of the particles, the thickness difference (ΔX_i) as a function of height (*i*) between the filaments of the PMMA suspension and the viscosity-matched silicone oil was measured, in an area spanning 350 μm up and down from the filament center (vertical axis = 0 in Figure 3.3.2. (a)). The coordinates of the thinning filament were extracted by MATLAB code. In order to extract the coordinate, the light intensity of each pixel was obtained from the images using MATLAB firstly. From the light intensity, the code found the location of the edge of the filament by using the difference in light intensity between the empty space (white color) and the filament (black color). Using the coordinates ΔX_i could be obtained. Then the root mean square ($\Delta X_{rms} = \sqrt{\frac{\sum_i (\Delta X_i)^2}{n}}$) of ΔX_i was calculated and plotted with the minimum neck diameter. Through this parameter, the effect of the particles on the shape of the filament surface was quantified.

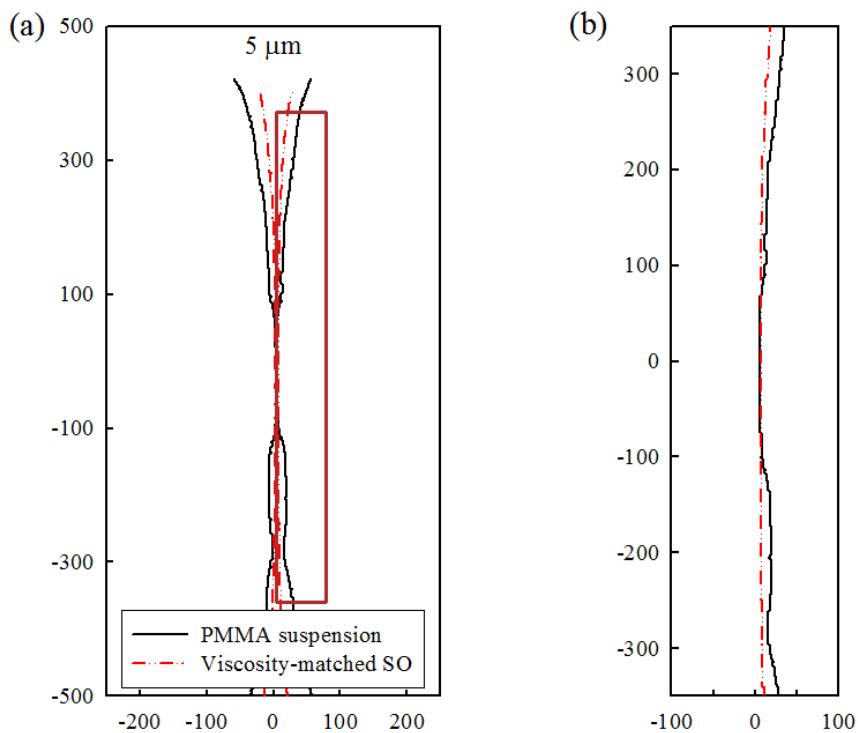

Figure 3.3.2. (a) Section for measuring the thickness difference (ΔX_i) between the filaments of the 20 wt% PMMA suspension and the viscosity-matched silicone oil at W=5 μm. (b) Expanded part of red box in (a).

3.3.3. Measurement of roughness of filament surface

The filament shape of the Newtonian fluid showed a saddle-like (parabolic in 2D image) and smooth pattern until pinch-off, whereas that of the PMMA suspension became rough when the filament was thinner in length scale of the particle diameter. To quantify the roughness of the filament surface, the error (ε) between the coordinate of the filament surface, spanning 350 μm up and down from the filament center (vertical axis=0 in Figure 3.3.3) and a fitting with a 2nd-order polynomial equation was measured. Because the shape of free surface of the PMMA suspension still kept a parabolic pattern, but the surface was rough. Then, root mean square ($\varepsilon_{rms} = \sqrt{\frac{\sum_i (\varepsilon_i)^2}{n}}$) of error was calculated and plotted as a function of the minimum neck diameter. The results were repeated three times. The coordinates of the filament surface were extracted with MATLAB.

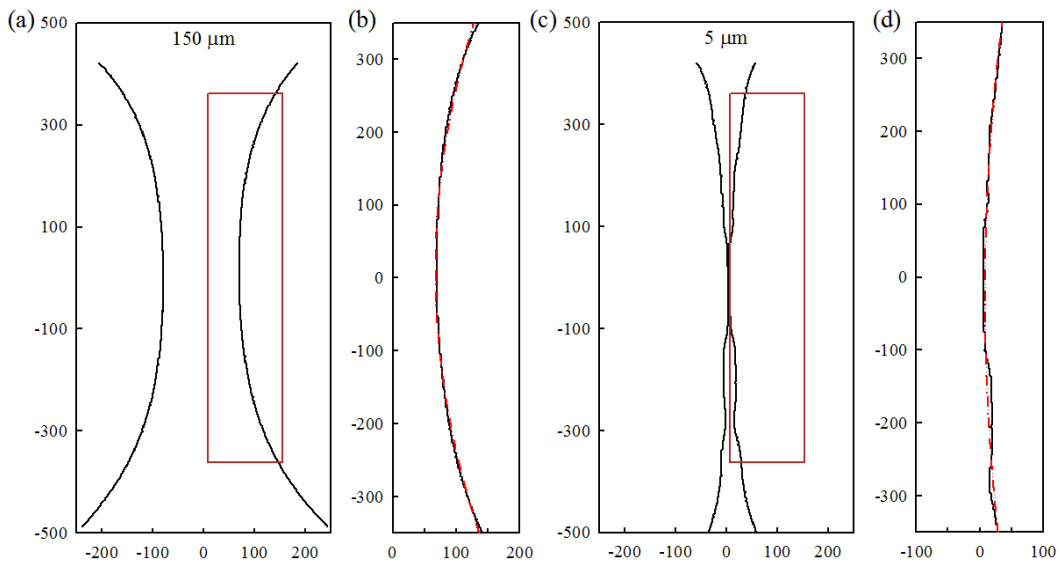

Figure 3.3.3. (a) Section to fit the free surface of the 20 wt% PMMA suspension (black solid line) with a 2nd-order polynomial equation (red dashed line) at W=150 μm, (b) expanded part of the red box in (a); (c) section at W=5 μm, (d) expanded part of the red box in (c). The axis is in μm.

3.3.4. Analysis of light intensity

The difference in the local concentration of the particles confined in the filament induced the non-uniform filament shape in the final stage of the thinning filament. Therefore, it was necessary to quantify the distribution of the particles. For that analysis, the light intensity in the central part of the filament (red box in Figure 3.3.4) was measured because the areas where the particles were present were dark, and the areas where the particles were absent were bright. The particle distribution was analyzed using the difference in light intensity. For this quantification, the distribution of the light intensity was obtained from the central part of the filament spanning a width of 3 pixel and a height of 512 pixel (5.82 μm×993.28 μm) as shown in Figure 3.3.4. The light intensity extracted from the black-and-white images was represented with numbers between 0 and 255. The light intensity 0 indicated black color, and that of 255 indicated white color. The representative light intensity at each height was calculated by averaging the light intensity of 3 pixels at the same height; approximately half of the particle diameter (10 μm) is in horizontal direction.

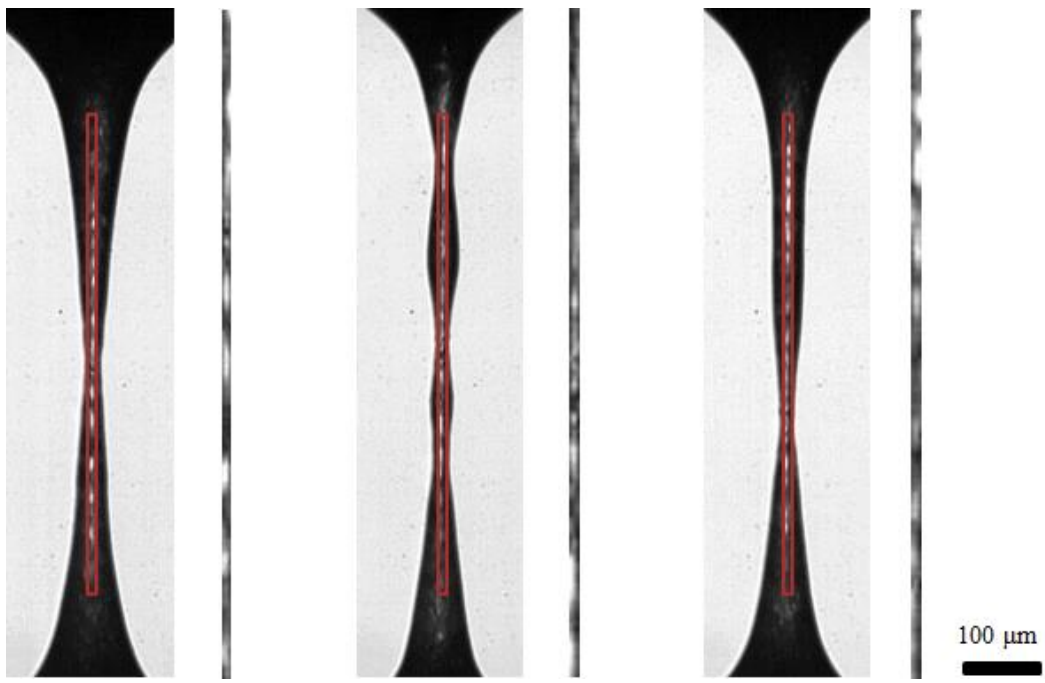

Figure 3.3.4. Section for measuring the light intensity from the snapshots of the filaments for the 20 wt% PMMA suspension at W=20 μm (3 different trials).

Chapter 4.

Results and discussion

4.1. Thinning dynamics of pure silicone oil

4.1.1. Effect of medium viscosity

First, the effect of the medium viscosity on the thinning dynamics of pure silicone oils was observed. Five silicone oils were prepared with different viscosities from 0.20 to 1.08 Pa s and with almost the same surface tension through mixing *SO-0.01* and *SO-10* at various ratios. The silicone oil properties are presented in Table 4.1.1. Figure 4.1.1 presents the time evolutions of the minimum neck diameters of the silicone oils. As depicted in Figure 4.1.1, the processing time required to breakup increases with the medium viscosity. It implies that the high medium viscosity decelerates the breakup of the thinning filament for Newtonian fluids. The thinning dynamics is governed by the competition among the capillary, inertia, and viscous forces. The capillary force (surface tension) is the driving force for the filament thinning, while the inertia and viscous forces provide resistance to the capillary force. The strong inertia and viscous forces caused by the increase in the medium viscosity decrease the breakup velocity.

Table 4.1.1. Silicone oil properties at various compositions of *SO-0.01* and *SO-10*.

Composition of *SO-0.01*	**Composition of *SO-10***	**η_{so} (Pa s)[a]**	**γ (mN/m)[b]**
0.7	0.3	0.20±0.01	20.5±0.1
0.6	0.4	0.40±0.01	20.5±0.1
0.55	0.45	0.58±0.01	20.6±0.1
0.5	0.5	0.84±0.01	20.7±0.1
0.45	0.55	1.08±0.01	20.7±0.1

a: medium viscosity of silicone oil

b: surface tension

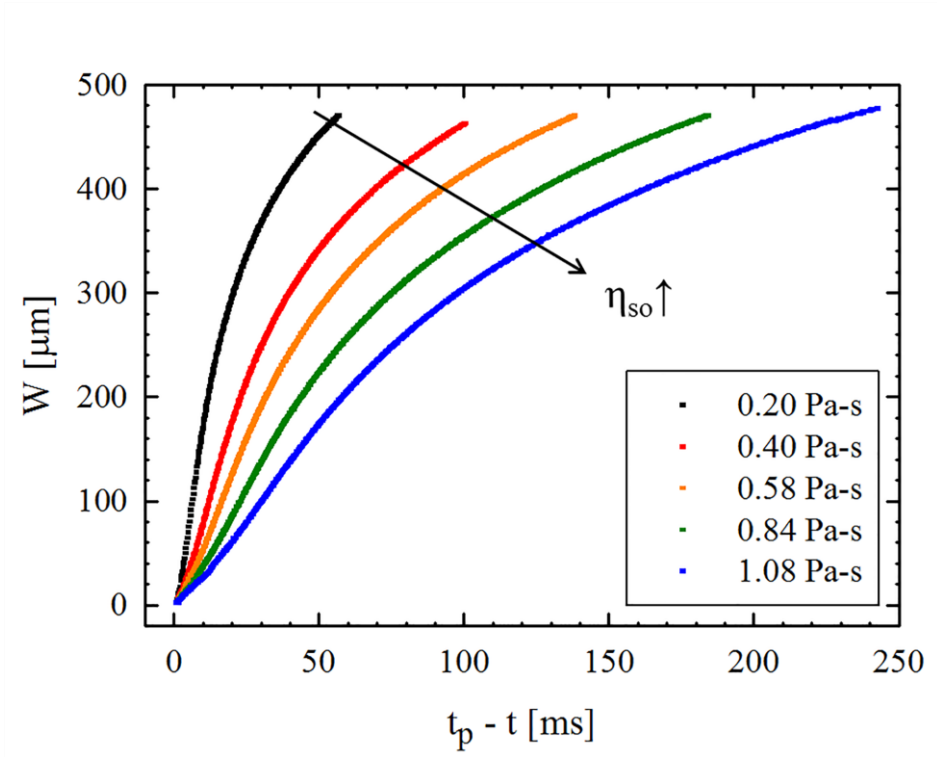

Figure 4.1.1. Time evolutions of the minimum neck diameter (*W*) of the pure silicone oils with various medium viscosities.

4.1.2. Final breakup velocity

In the final stage of the breakup process (W<150 μm from Figure 4.1.1), the minimum neck diameter decreases almost linearly as shown in Figure 4.1.2. That is, the breakup velocity is almost constant in that regime. The regime is often called 'Stokes regime' (Papageorgiou 1995; Rothert *et al*. 2003), in which the minimum neck diameter decreases linearly and the influence of inertia can be neglected. However, the curve with the viscosity larger than 0.6 Pa s is slightly convex downward because of inertia force induced by the stagnation point of the filament (a central part of the filament). However the influence of the inertia force is not strong.

The final breakup velocity at W<150 μm was obtained by calculating the slope of each curve as depicted in Figure 4.1.3. The breakup velocity in the Stokes regime decreases with the medium viscosity. It is plotted as a function of γ/η (γ : surface tension, η : medium viscosity), and shows a linear curve as shown in Figure 4.1.4. This tendency is well matched with the calculated values by the theoretical prediction, Equation (4.1.1) (McKinley and Tripathi 2000). It should be noted that the silicone oil shows an almost constant breakup velocity in the final stage and the medium viscosity determines the thinning dynamics of the filament.

$$V = 0.1418 \times \frac{\gamma}{\eta}. \qquad (4.1.1)$$

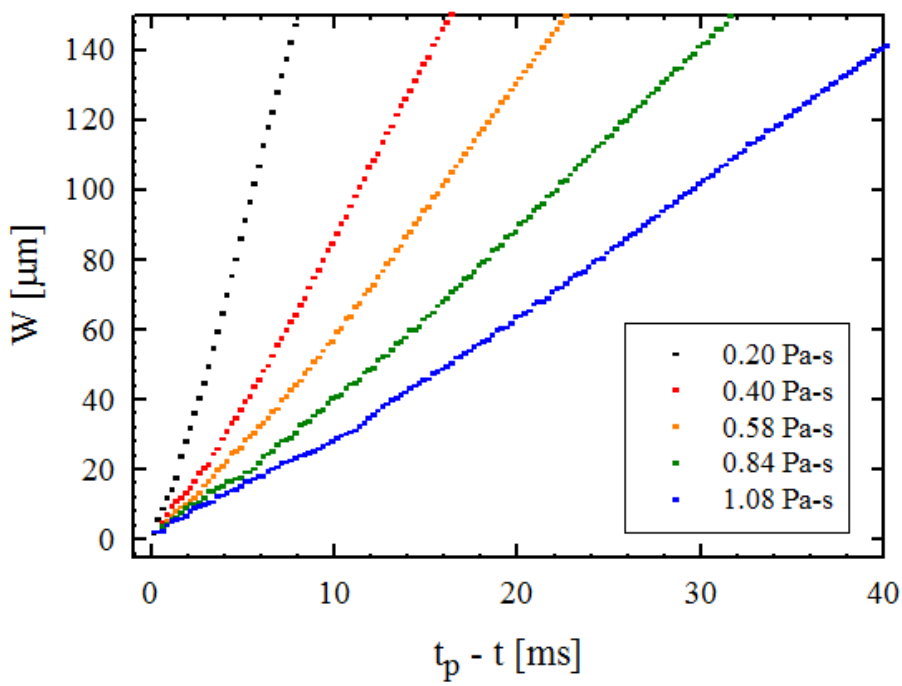

Figure 4.1.2. Time evolutions of the minimum neck diameter (*W*) of the pure silicone oils with various medium viscosities. (*W*< 150 μm in **Figure 4.1.1**).

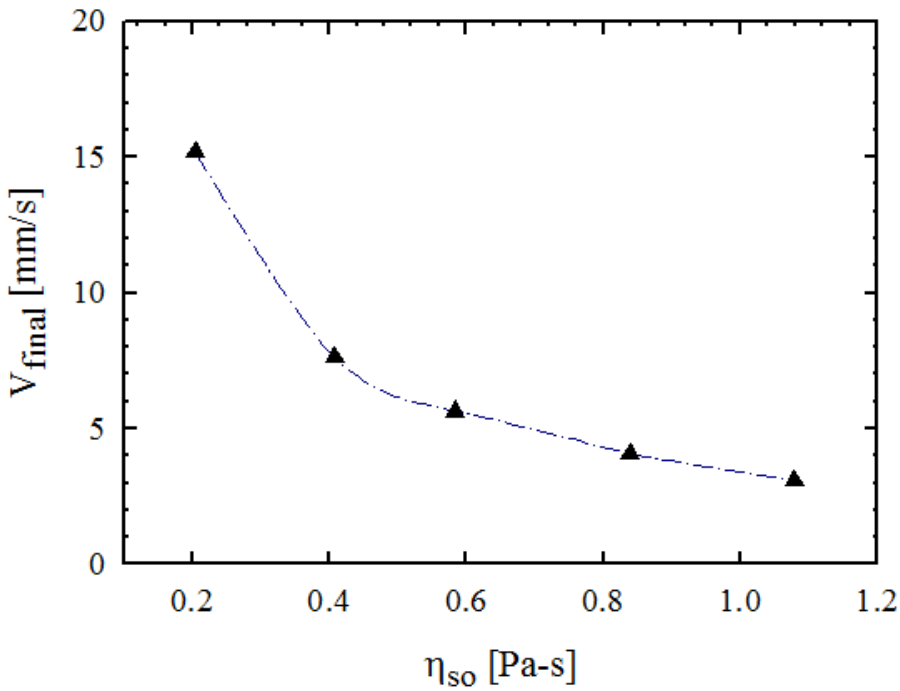

Figure 4.1.3. Breakup velocity (V_{final}) of the silicone oils in the final stage of breakup as a function of the medium viscosity.

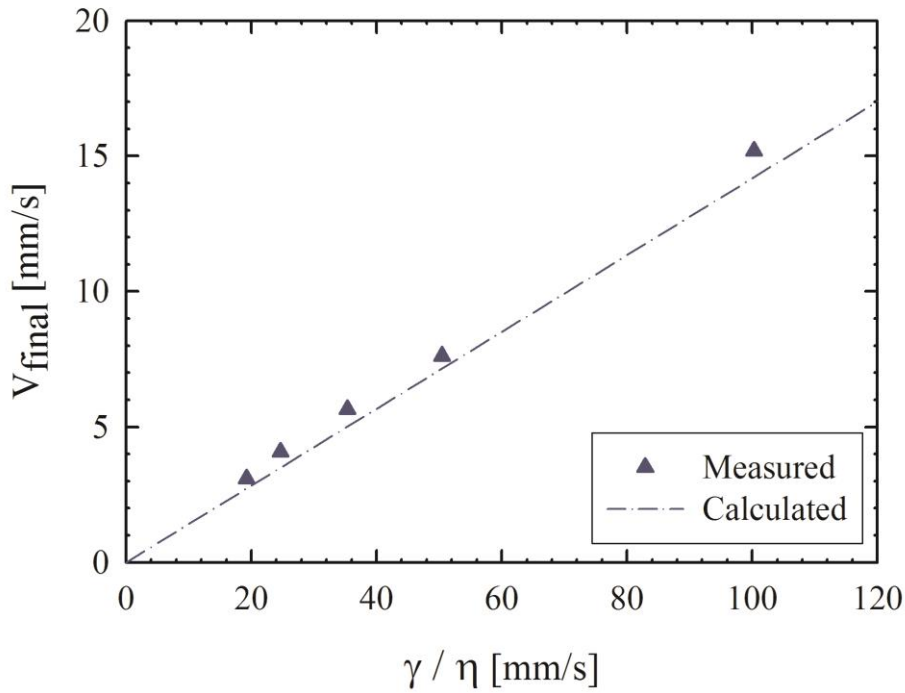

Figure 4.1.4. Final breakup velocity (V_{final}) of the silicone oils in Stokes regime (W<150 μm) as a function of γ/η . (γ : surface tension, η : medium viscosity).

4.2. Filament breakup of silicone oil/PMMA suspensions

4.2.1. Effect of particle concentration

In order to investigate the effect of the particles on the filament breakup process, 10 μm PMMA particles were suspended in *SO-0.40* up to 20 wt%. As illustrated in Figure 3.1.1, the effective viscosity of the PMMA suspension increased with the particle concentration. The addition of 20 wt% PMMA particles increased the effective viscosity to 0.71 Pa s. From Figure 4.2.1, the effect of the particle concentration on the time evolution of the minimum neck diameter of the PMMA suspensions was observed.

Firstly, when the minimum neck diameter is larger than 200 μm, the time required to reduce the minimum neck diameter from 850 μm to 200 μm increases with increases in the particle concentration. The breakup velocity is reduced as the particle concentration increases because the addition of particles increases the effective viscosity of the suspension. This tendency has already been reported (Furbank and Morris 2007; Bonnoit *et al*. 2012), and the thinning dynamics is governed by the effective viscosity of the suspension in this regime; thus, it has been named the ‘effective regime’.

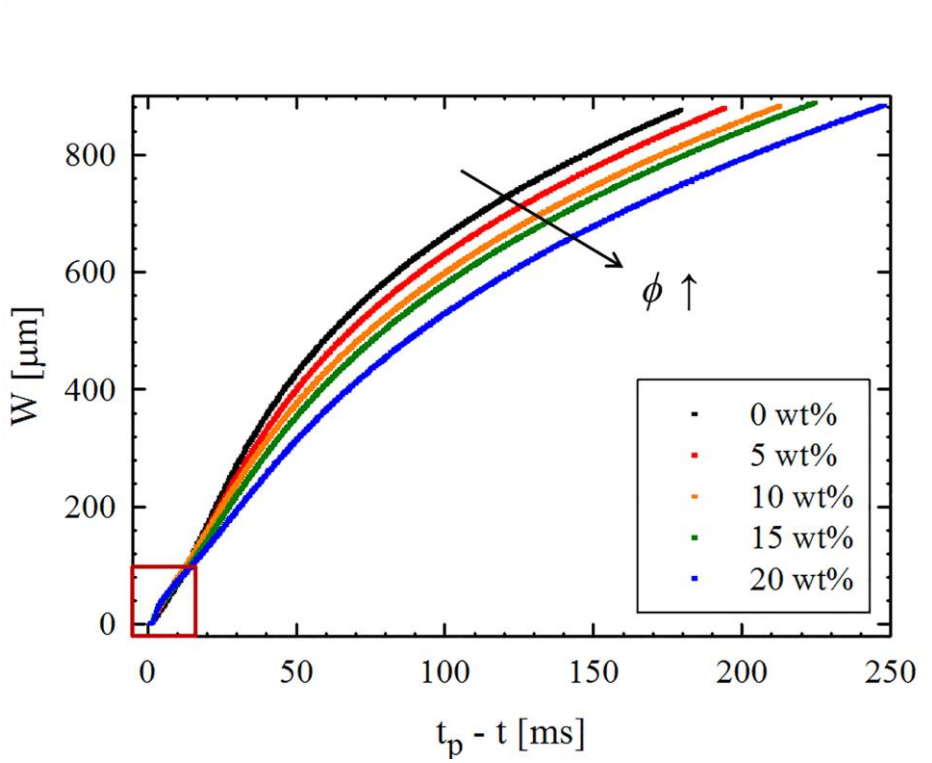

Figure 4.2.1. Time evolutions of the minimum neck diameter (*W*) for PMMA suspensions at various particle concentrations (0~20 wt%).

When the minimum neck diameter is less than 100 μm (red box in Figure 4.2.1), the thinning dynamics of the PMMA suspensions seem to be independent of the particle concentration. In other words, they appear to be governed only by the suspending medium even though they have different effective viscosities. This phenomenon differs significantly from the previous result in *Section 4.1*, where the medium viscosity affects the thinning filament of the pure silicone oils until the pinch-off point. This tendency has also been reported in Bonnoit *et al*. (2012), in which the authors hypothesized that the thinning dynamics in this regime was governed by the properties of the suspending medium regardless of the particle concentration. This indicates that the addition of particles does not further affect the thinning dynamics.

However, according to the closer observations in the region of t_p–t<30 ms in Figure 4.2.1, the curves do not collapse into a single curve as seen in Figure 4.2.2. The filaments become thinner with different slopes (breakup velocities) as approaching the pinch-off. The slopes change around W=5 D (50 μm, D: the particle diameter, 10 μm), and the degree of change increases further with increase of particle concentrations. That is, the PMMA suspensions with various particle concentrations have different breakup velocities in the final stage of the breakup process, unlike the Newtonian fluids. According to the results observed in the μm-length scale, it can be confirmed that the particles still affect the thinning dynamics of the filament in the "interstitial regime" (near W~5 D).

Two important contributions of the particles in the final stage are the deceleration and acceleration of the breakup process. These regimes are separated to before and after W=5 D as depicted in Figure 4.2.2, and the breakup velocity

changed at approximately W=5 D. When the minimum neck diameter is larger than 5 D, the breakup velocity is reduced with increases in the particle concentration. When the filament becomes thinner than W=5 D, the particles increase the breakup velocity. Figure 4.2.3 presents the transition of the breakup velocities before and after W=5 D. For the silicone oil (ϕ=0 wt%, ϕ: particle concentration [wt%]), the breakup velocity in the range 10 μm<W<50 μm is lower than that for 50 μm<W<200 μm. As the particle concentration increases, the breakup velocity in the 10 μm<W<50 μm range increases and it decreases in 50 μm<W<200 μm. The breakup velocities at ϕ=3 wt% in both regimes are almost identical and the difference between the regimes increases with increases in the particle concentration. In conclusion, it is verified that the particles affect the dynamics of the thinning filament in the final stage by decelerating the breakup process before W=5 D (50 μm) and through accelerating the final stage of the filament breakup for W<5 D.

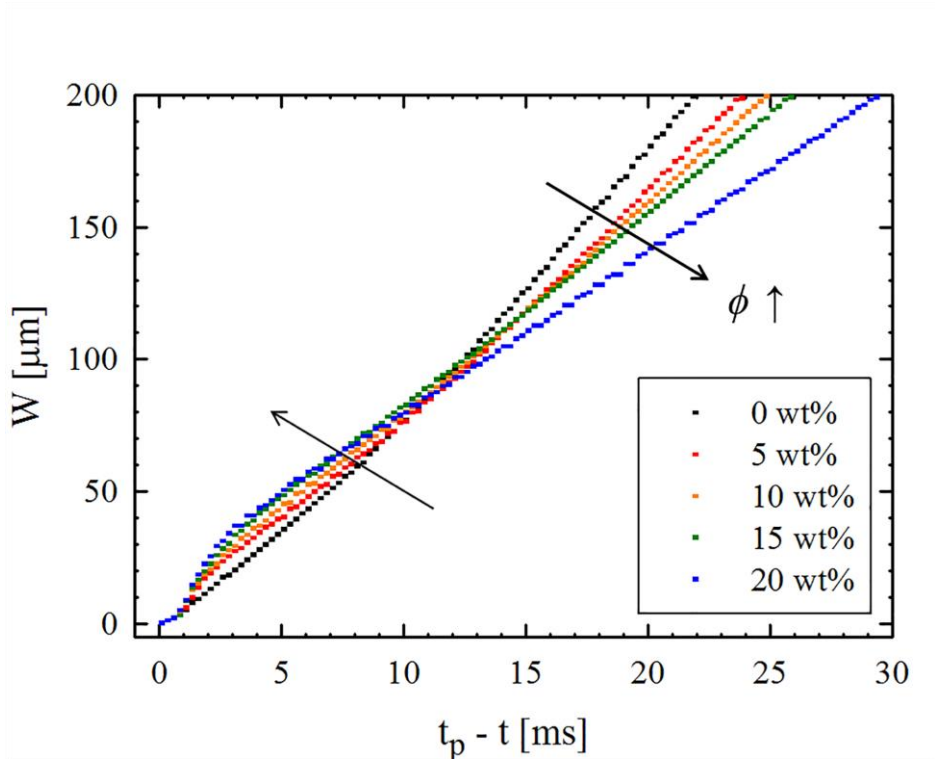

Figure 4.2.2. Time evolutions of the minimum neck diameter (*W*) for the PMMA suspensions at various concentrations of the PMMA particle (0~20 wt%) in the final stage.

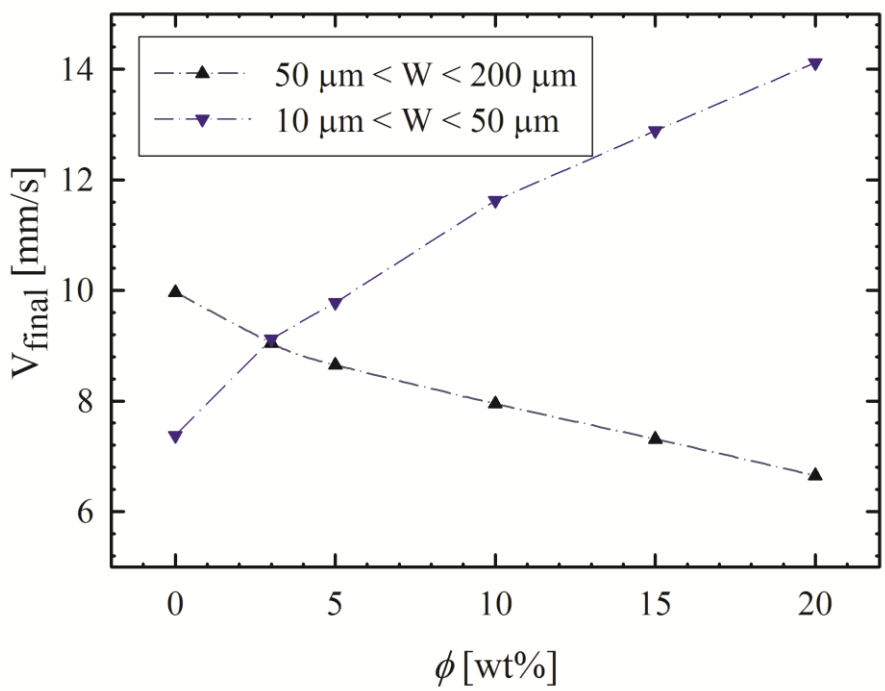

Figure 4.2.3. Final breakup velocities (V_{final}) for the PMMA suspensions at various particle concentrations in the final stage.

4.2.2. Comparison with viscosity-matched silicone oil

In order to investigate the effect of the particles on the filament breakup, a 20 wt% PMMA suspension and a silicone oil having the same viscosity and surface tension with the PMMA suspension were prepared for clarifying the effect of the particles without critical differences in the properties. The viscosity-matched silicone oil was made through mixing two silicone oils, *SO-0.01* and *SO-10* at a ratio of 54:46 (wt%). The viscosity was 0.71 Pa s and the surface tension was 20.5 mN/m. Because the viscosity and surface tension govern the thinning dynamics of the filament breakup, the effect of the particles on the filament breakup can be observed separately by comparing these fluids. Figure 4.2.4 presents the time evolution of the minimum neck diameter of these two fluids.

When $W>35\ D$ (350 μm), the thinning dynamics is dependent on the effective viscosity of the fluid. Thus, the minimum neck diameter for both the PMMA suspension and viscosity-matched silicone oil are equivalent and their breakup velocities are almost the same. In this regime, the particles decelerate the breakup process due to the increase in the effective viscosity.

When the filament becomes thinner than 35 D, the thinning dynamics of the 20 wt% PMMA suspension and viscosity-matched silicone oil shows differences even though they have the same viscosity and surface tension. In addition to the increase in the effective viscosity, the particles decrease the breakup velocity more than the viscosity-matched silicone oil because the particles confined in the narrow filament channel disturb the flow of the thinning filament under the extensional flow. Therefore, it can be confirmed that the particles decelerate the breakup process and

this tendency is observed until the minimum neck diameter of approximately 5 D (50 μm).

Close to the pinch-off at W<5 D, the particles do not decrease the breakup velocity, but rather they accelerate the breakup. This is the acceleration regime. When we focus on the thinning dynamics of the viscosity-matched silicone oil, the curve of the minimum neck diameter is slightly convex downward. The breakup velocity in this regime is slightly lower than that in W>5 D, and this result can be observed in Figure 4.2.3 at ϕ=0 wt%. This deceleration is induced via the inertia force at the stagnation point which is the central part of the filament without a velocity profile from the initial stage of the breakup process. However, the particles increase the breakup velocity as the filament becomes thinner than approximately five times of the particle diameter. The individual PMMA particles with a finite size of 10 μm begin to have a role and they exert a significant influence on the thinning behavior. This is the "finite-size effects of individual particles", and this effect has been reported in previous researches (Furbank and Morris 2004; Furbank and Morris 2007; McIlroy and Harlen 2014).

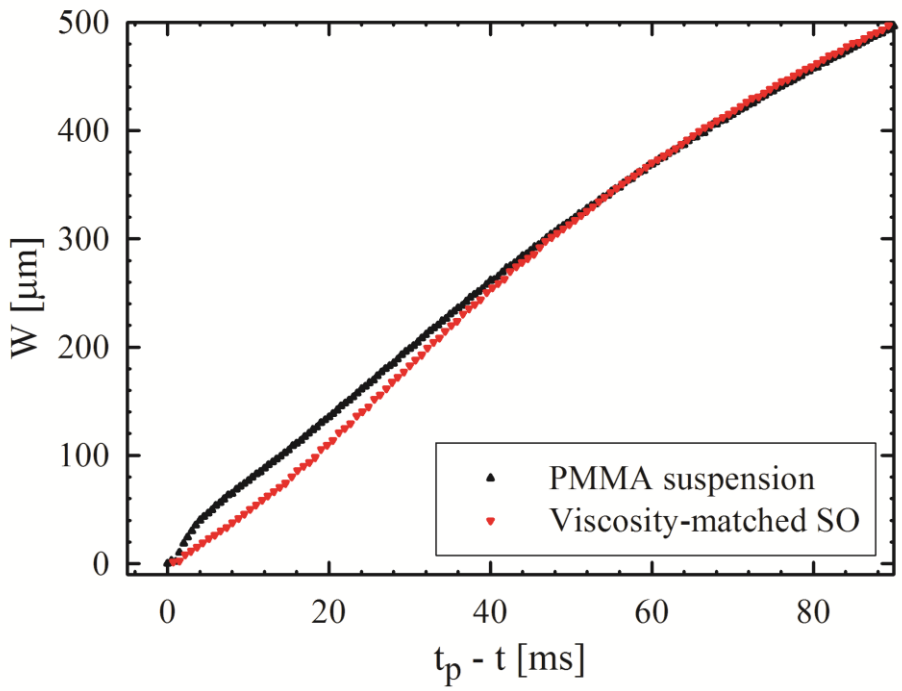

Figure 4.2.4. Time evolutions of the minimum neck diameter (*W*) for the 20 wt% PMMA suspension and viscosity-matched silicone oil.

From Figure 4.2.4, the breakup velocity (V) of the thinning filament for both the 20 wt% PMMA suspension and viscosity-matched silicone oil was obtained. The breakup velocity was calculated using the simple finite difference method after averaging the data in Figure 4.2.4 in order to reduce small fluctuations. As seen in Figure 4.2.5, the breakup velocities of the PMMA suspension and viscosity-matched silicone oil are almost the same for W>35 D. However, as the filament becomes thinner under W=35 D, the breakup velocity of the 20 wt% PMMA suspension is lower than that of the viscosity-matched silicone oil until W=10 D. As the filament becomes further thinner, the difference is reduced and there is a transition at approximately W=5 D. Finally, the breakup velocity of the PMMA suspension increases significantly compared with the constant breakup velocity of the viscosity-matched silicone oil for W<5 D. As explained previously, the particles induced the acceleration of the breakup in this stage. Moreover, the breakup velocity of the PMMA suspension at W=10 D is approximately 15% lower than that of the viscosity-matched silicone oil. This is significantly larger than the error bound of the experiments, i.e. 1~2%; thus, it cannot be ignored. This indicates that the particles affect the thinning filament, while the particles confined in the thinning filament disturb the flow in the final stage.

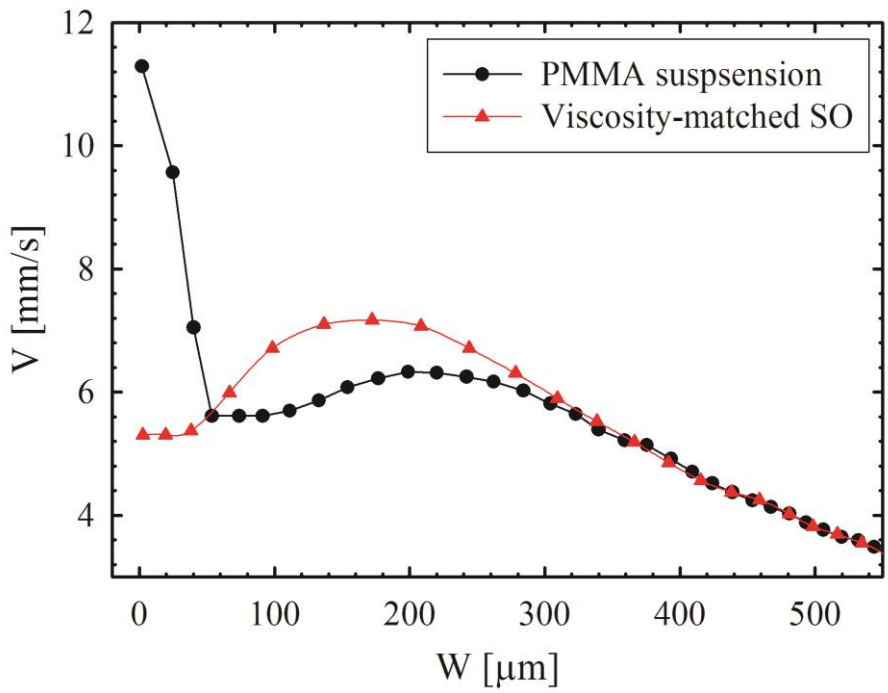

Figure 4.2.5. Breakup velocities of the 20 wt% PMMA suspension and viscosity-matched silicone oil.

4.3. Effect of particles on filament shape

4.3.1. Comparison of silicone oil/PMMA suspension and viscosity-matched silicone oil

The particles affect not only the thinning dynamics, but also the shape of the free surface. The filament shape of the 20 wt% PMMA suspension was compared with that of the viscosity-matched silicone oil (SO), which had the same viscosity and surface tension as the PMMA suspension. Figure 4.3.1 illustrates the shape of the free surface for the PMMA suspension and viscosity-matched silicone oil. The scale in Figure 4.3.1 is the actual length scale of the filament in μm.

The filament shapes for the PMMA suspension and the viscosity-matched silicone oil are almost the same until the minimum neck diameter becomes 10 D (100 μm) because they have the same viscosity and surface tension. The particles do not have any influence on the filament shape in that regime (W>10 D).

However, the filaments begin to show differences in shapes when the minimum neck diameter is less than 10 D. The filament of the viscosity-matched silicone oil becomes thinner until pinch-off, while maintaining a parabolic and smooth surface pattern. The filament of the PMMA suspension becomes thinner until W=2 D while still keeping a parabolic shape, but both ends of the filament are thicker than that of the silicone oil. When the filament of the PMMA suspension is thinner under W=2 D, the filament shape becomes rough, not parabolic nor smooth. The differences in the filament shape increase as the filaments become even thinner.

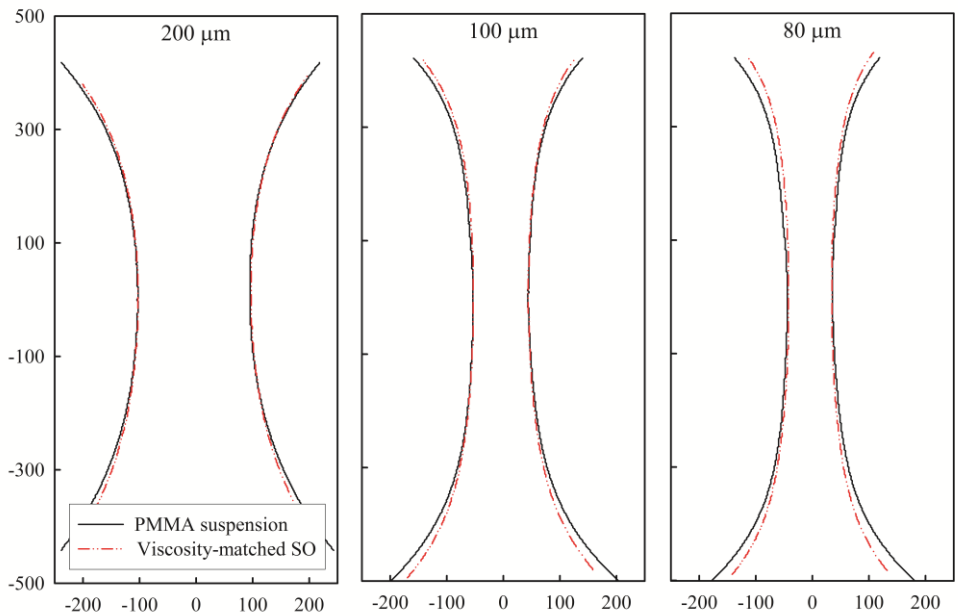

Figure 4.3.1. (a) Comparison of the filament shapes for the 20 wt% PMMA suspension and the viscosity-matched silicone oil at the same minimum neck diameter for 200, 100, 80 µm (the numbers on the top of each graph). The axis is in µm.

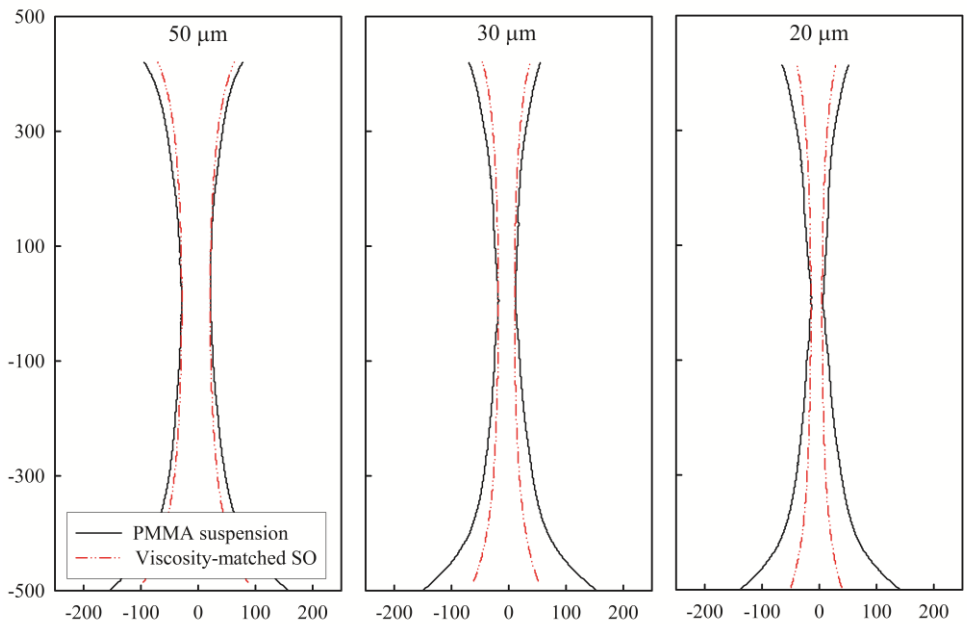

Figure 4.3.1. (b) Comparison of the filament shapes for the 20 wt% PMMA suspension and the viscosity-matched silicone oil at the same minimum neck diameter for 50, 30, 20 µm (the numbers on the top of each graph). The axis is in µm.

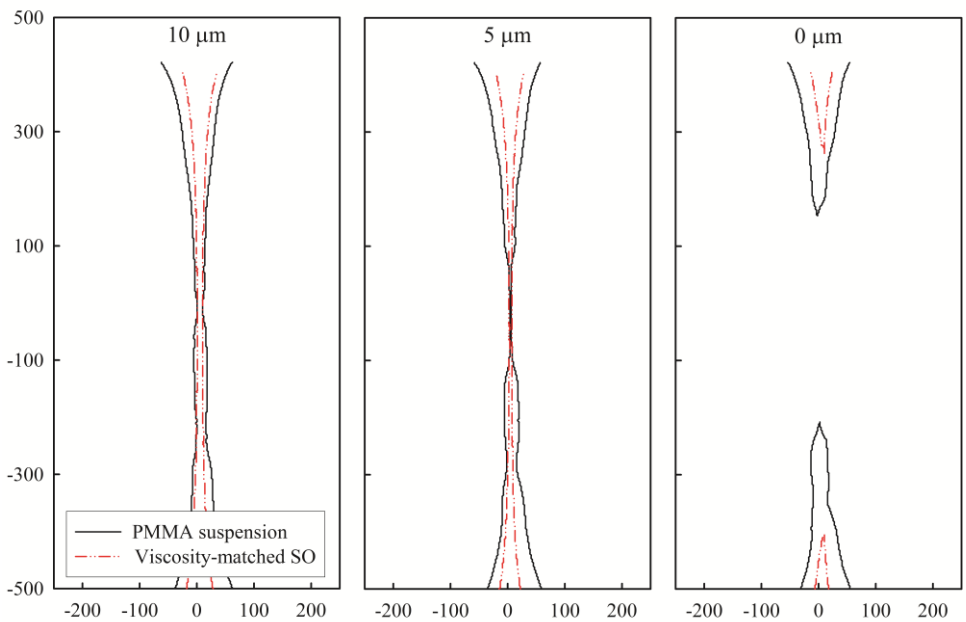

Figure 4.3.1. (c) Comparison of the filament shapes for the 20 wt% PMMA suspension and the viscosity-matched silicone oil at the same minimum neck diameter for 10, 5, 0 µm (the numbers on the top of each graph). The axis is in µm.

As shown in Figure 4.3.1. (a), the particles begin to affect the filament shape when the filament becomes thinner than W=10 D (100 μm). The effect of the particles is quantified through root mean square ($\Delta X_{rms} = \sqrt{\frac{\sum_i (\Delta X_i)^2}{n}}$, defined in *Section* 3.3.2) of thickness difference between the two filaments of the fluids (ΔX_i) as shown in Figure 4.3.2.

The two filaments become thinner until W=10 D while maintaining a low ΔX_{rms} of approximately 2.85~3.29 μm, as shown in Figure 4.3.2. In other words, the shapes of the two filaments are almost the same, which indicates that the particles minimally affect the filament shape in the regime of W>10 D. However, ΔX_{rms} begins to increase when the minimum neck diameter reduces to less than 10 D, and it fluctuates significantly when the minimum neck diameter of the filament is around 2 D (20 μm). The sudden change is induced by the rough filament of the PMMA suspension as shown in Figure 4.3.1. (b), (c) for W≤2 D.

The sudden change of ΔX_{rms} for W≤2 D shows poor reproducibility, as in Figure 4.3.3, which shows the results repeated for three times. The reproducibility of ΔX_{rms} is very good when the minimum neck diameter is larger than 2 D. However, ΔX_{rms} is rarely reproducible when the filament becomes thinner than W=2 D. In conclusion, the added particles rarely affect the filament shape until W=10 D. The particles begin to affect the filament shape when the minimum neck diameter is reduced to less than 10 D, and they induce a filament shape in which both ends are thick while being parabolic in shape. When the filament becomes thinner than W=2 D, the particles lead to non-uniform behavior close to the

breakup point of the filament. This is a random pinch-off behavior. In this way, the added particles not only affect the breakup velocity in the final stage of filament breakup but also induce complicated and heterogeneous behavior in the filament shape. The heterogeneity increases as approaching the pinch-off.

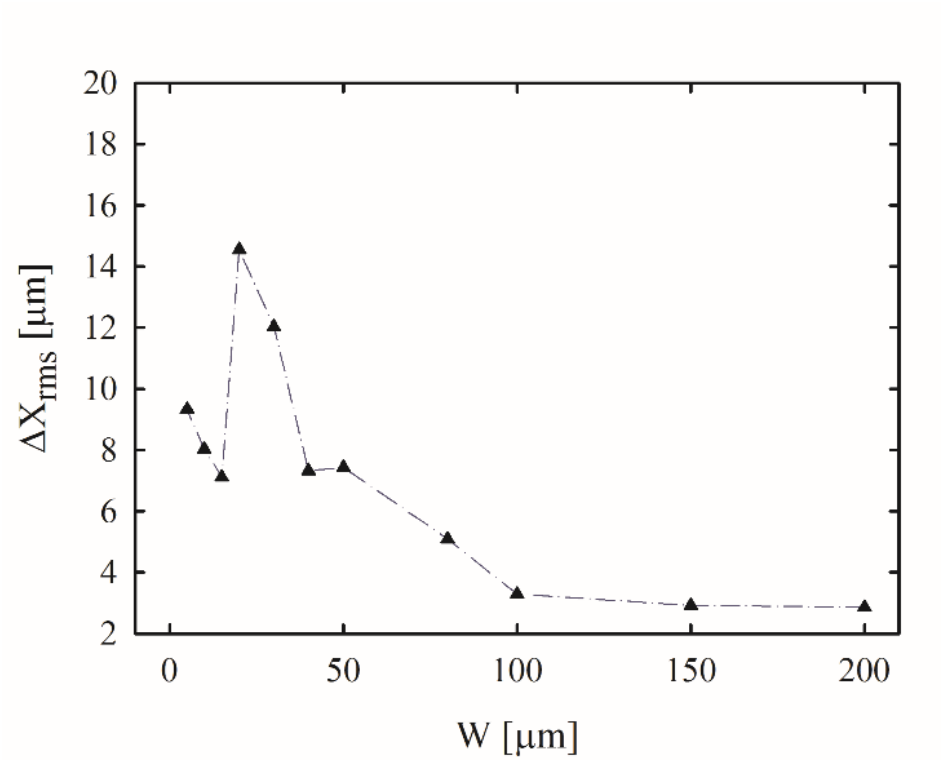

Figure 4.3.2. Root mean square (ΔX_{rms}) of the thickness difference between the filaments of the 20 wt% PMMA suspension and the viscosity-matched silicone oil at the same minimum neck diameter (W).

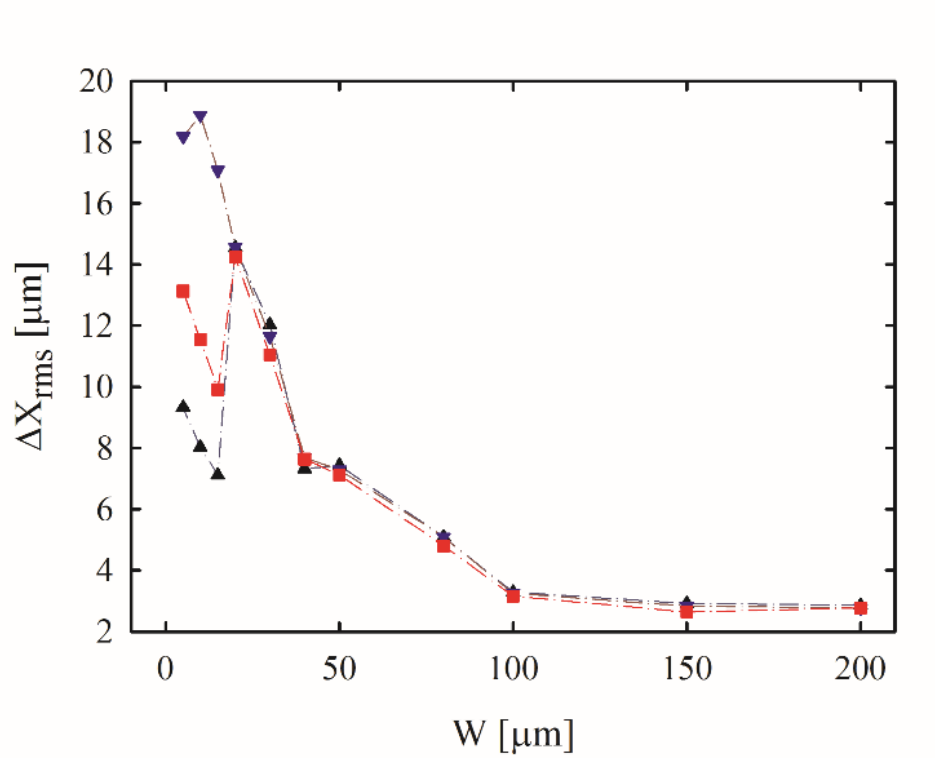

Figure 4.3.3. Reproducibility of the root mean square (ΔX_{rms}) of the thickness difference between the filaments of the 20 wt% PMMA suspension and the viscosity-matched silicone oil at the same minimum neck diameter (W). The results were repeated three times.

4.3.2. Effect of particles on roughness of filament surface

As explained in *Section 4.3.1* the filament surface of the 20 wt% PMMA suspension is rough when the minimum neck diameter of the filament reduces to less than 2 D (20 μm). The roughness is quantified using root mean square ($\varepsilon_{rms} = \sqrt{\frac{\sum_i (\varepsilon_i)^2}{n}}$, defined in *Section* 3.3.3) of error (ε) between a fitting with a 2nd-order polynomial equation and the coordinate of the filament surface.

In Figure 4.3.4, the ε_{rms} of the PMMA suspension and the viscosity-matched silicone oil are almost the same when the minimum neck diameter is larger than 3 D (30 μm), which means that the shape of the filament is well-described by a 2nd-order polynomial equation. As confirmed in Figure 4.3.1, the particles begin to affect the filament shape when the filament becomes thinner than W=10 D. However, the ε_{rms} for the PMMA suspension and the viscosity-matched silicone oil are almost the same when the minimum neck diameter is larger than 3 D. It means that in the regime of 3 $D \leq W \leq 10$ D, the filament of the PMMA suspension becomes thinner while maintaining a parabolic surface even though the ends of the filament are thicker than that of the viscosity-matched silicone oil. Thus, the ε_{rms} for the PMMA suspension and the viscosity-matched silicone oil do not show critical differences.

However, the ε_{rms} of the PMMA suspension begins to increase rapidly compared to that of the silicone oil as the minimum neck diameter of the filament reduces down to 2 D. The rapid increase is induced by the rough thinning filament of the PMMA suspension as depicted in Figure 4.3.1 for $W \leq 2$ D. The filament

shape of the PMMA suspension is not parabolic and smooth in that regime ($W \leq 2D$). An additional point to be noted is the error bar of ε_{rms} in Figure 4.3.4 for the PMMA suspension. The error bar of ε_{rms} begins to increase when the minimum neck diameter is less than 2 *D*. This is because the thinning filament has a random surface profile close to the pinch-off under $W=2D$ as shown in *Section 4.3.1*.

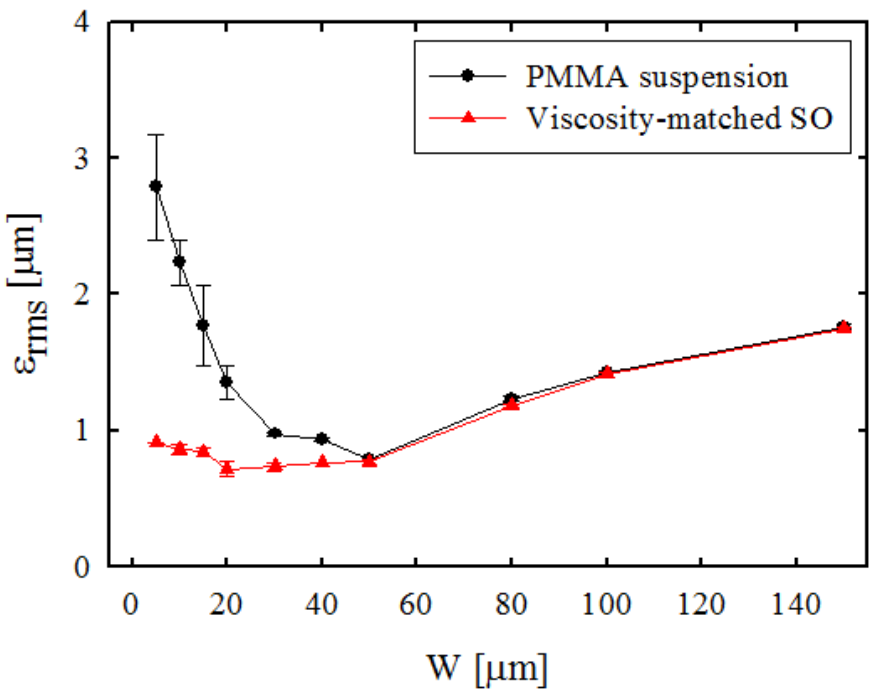

Figure 4.3.4. Root mean square error (ε_{rms}) obtained by fitting with a 2nd-order polynomial equation, for the filaments of the 20 wt% PMMA suspension and the viscosity-matched silicone oil as a function of the minimum neck diameter (W). The results were repeated for three times.

4.4. Heterogeneity in filament breakup process

4.4.1. Random pinch-off behavior

According to the previous *Sections 4.3*, it is clear that the filament of the PMMA suspension becomes heterogeneous when the filament becomes thinner than W=2 D. In particular, it becomes very non-uniform close to the pinch-off. Figure 4.4.1 illustrates the filament shape of the two fluids at pinch-off. Each graph depicts snapshots of the thinning filaments for three repetitions.

The reproducibility of the pinch-off shape is almost perfect for the Newtonian fluid, as shown in Figure 4.4.1 (a). The three-overlaid snapshots appear to fit within a single figure, which means that the filament shape of the Newtonian fluid is uniform during pinch-off. This tendency is in accordance with the previous researches on the filament thinning process of Newtonian fluids (Papageorgiou 1995; Eggers 1997; Rothert *et al*. 2003). They showed that the final stage of the filament breakup including the pinch-off shape is determined by the properties of the fluid only, viscosity and surface tension, even though the external conditions can have an influence in the initial stage, such as the volume of a loaded sample. However, for the PMMA suspension (Figure 4.4.2 (b)), the results are not reproducible at all, and multiple samples exhibit different shapes at pinch-off. The added particles induce the random pinch-off behavior.

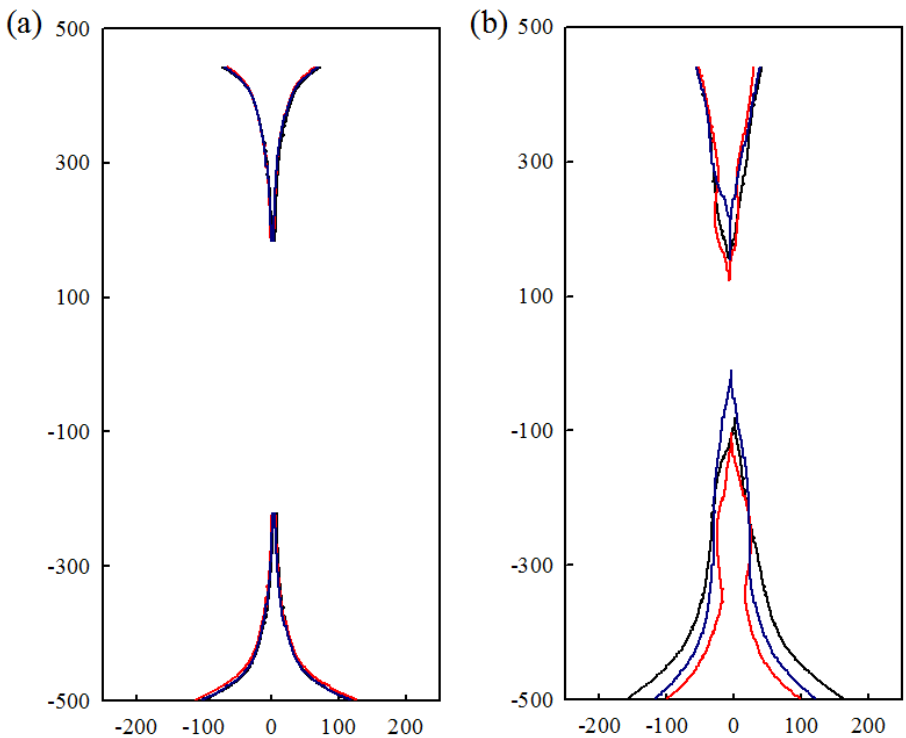

Figure 4.4.1. The filament shapes for (a) the viscosity-matched silicone oil and (b) the 20 wt% PMMA suspension at pinch-off. The axis is in μm. The results were obtained three times and are plotted in each graph.

Figure 4.4.2 shows the snapshots of three different filaments for the 20 wt% PMMA suspension when the minimum neck diameter of the filaments is 2 *D* (20 μm). The position of the thinnest part and the surface shape of the filament are not uniform at all. This heterogeneity begins to appear as the filament becomes thinner than $W=2D$. When the filament is thin in the length scale of the particle diameter, the particles influence filament thinning, which is considered to be the 'finite size effect of the individual particle' (Furbank and Morris 2004; Furbank and Morris 2007; McIlroy and Harlen 2014). However, since the local concentration of the particles confined in the filament is not uniform, the randomness induces the heterogeneous pinch-off process.

As can be seen in Figure 4.4.2, the areas where particles are not present are bright because backlight can pass through the filament, while the areas with particles are dark. The bright and dark regions are randomly distributed. This means that the particles confined in the thinning filament are not uniformly distributed. Because the particles are distributed randomly, the thick part of the filament having more particles and the thin part with fewer particles are also randomly distributed. In practice the particles are distributed non-uniformly even when the filament is thick. The particles distributed randomly induce the local differences in particle concentration in the thinning filament when the filament becomes thin comparable to the particle size. The local randomness of the particles leads to a non-uniform filament shape as seen in Figure 4.4.2. Differences in filament shape between the PMMA suspension and the viscosity-matched silicone oil are not observed for $W>3D$. In conclusion, the random distribution of the particles leads to the heterogeneous filament thinning behavior in the final stage of

the breakup process when the filament becomes thinner than $W=2\,D$.

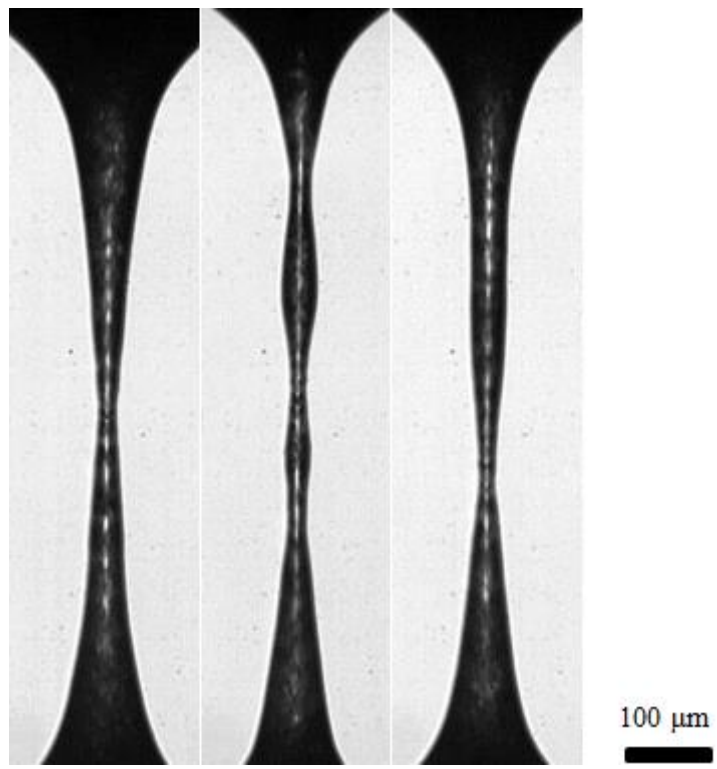

Figure 4.4.2. Snapshots of the filaments for the 20 wt% PMMA suspension at W=20 μm.

4.4.2. Random distribution of particles

The light intensity in the central part of the filament was measured in order to quantify the distribution of the particles confined in the filament. Figure 4.4.3 shows the change of light intensity for filaments of the 20 wt% PMMA suspension. At W=30 D (300 μm), the light intensity is very small, and close to zero, because the backlight can not pass through the thick filament comprised of multiple layers of particles. However, when the filament becomes thinner, the light intensity begins to increase at the center (Height=0 from Figure 4.4.3) of the filament. Under W=10 D (100 μm), the light intensity further increases and begins to fluctuate. The fluctuation grows as the minimum neck diameter of the filament reduces to 2 D. In this graph, the light intensity with large number indicates particle-free region (empty space) and the small number means the particle-rich region.

However, the light intensity shows poor reproducibility under W=10 D as seen in Figure 4.4.4. Figure 4.4.4 presents the reproducibility of the light intensity for the PMMA suspension with the minimum neck diameter. When the filament is thick over W=30 D, the light intensity have high reproducibility and it is still high until W=15 D even though some fluctuations at Height=0. However, when the filament becomes thinner under W=10 D, the fluctuation begins to increase and fluctuate non-uniformly. That is, the distribution of the particles confined in the filament is randomized with decrease of the minimum neck diameter in final stage of the breakup process. The randomness of the particles induces random shape of filament surface, random pinch-off.

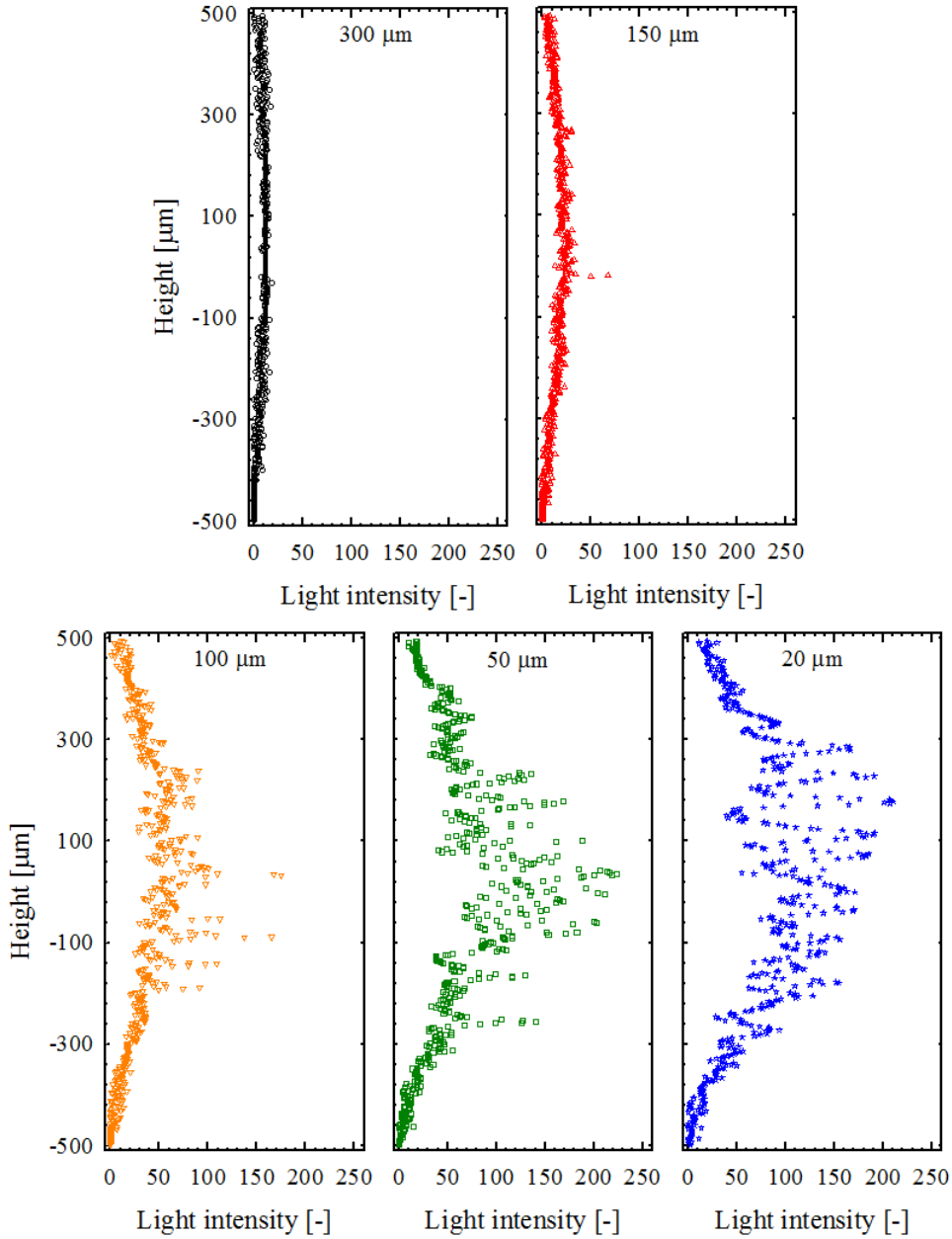

Figure 4.4.3. Light intensity distribution of a filament of the 20 wt% PMMA suspension. The numbers on the top of each graph are the minimum neck diameter.

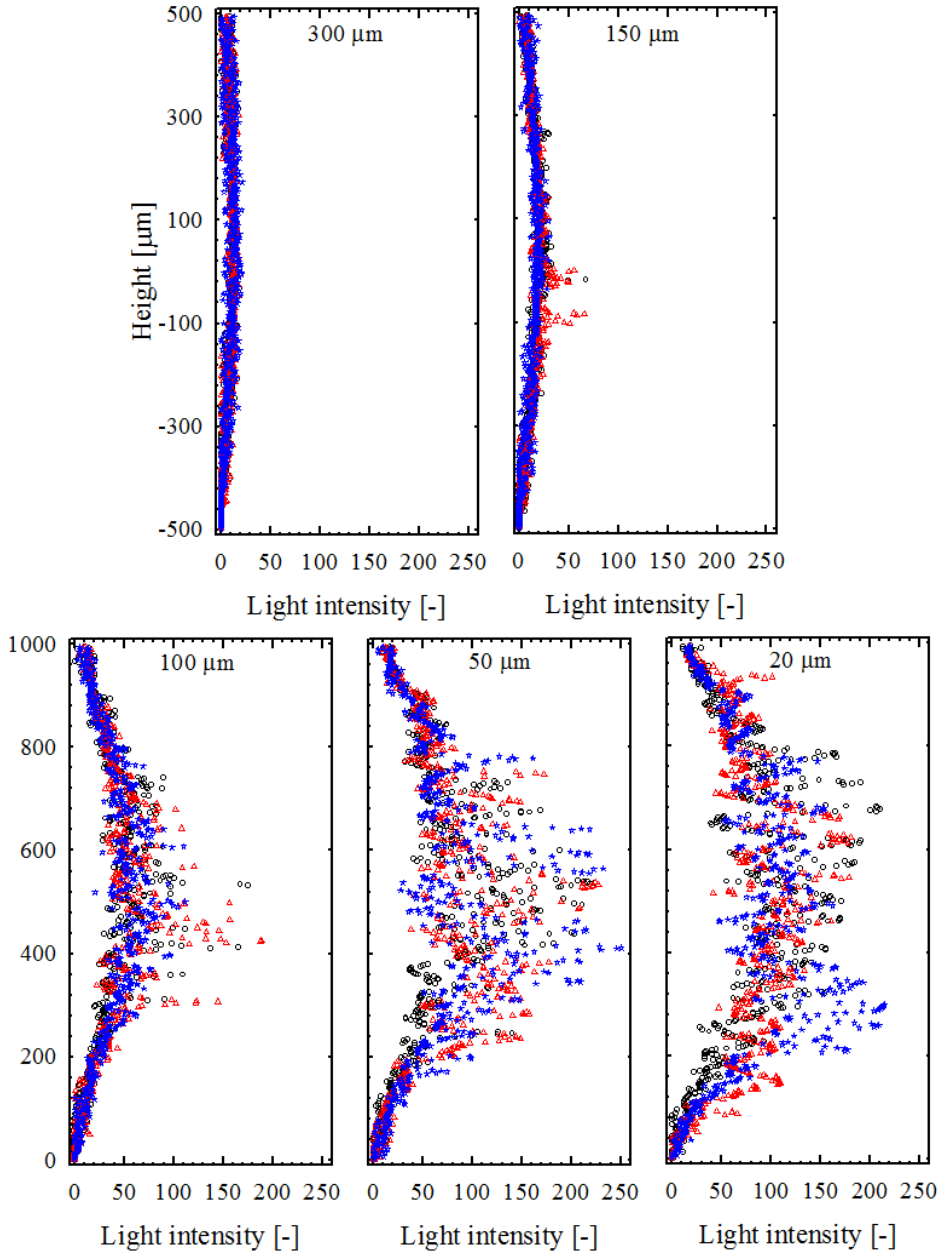

Figure 4.4.4. Reproducibility of light intensity distribution of a filament of the 20 wt% PMMA suspension. The numbers on the top of each graph are the minimum neck diameter.

From this graph, the distribution of the particles confined in the central part of the filament can be quantified. The distribution can be fitted well by a Gaussian probability distribution function with 4 parameters as defined in Equation (4.4.1). The parameters used for fitting are displayed in Table 4.4.1.

$$y = y_0 + ae^{\left[-0.5\left(\frac{x-x_0}{b}\right)^2\right]}. \quad (4.4.1)$$

When W=30 D (300 μm), the light intensity matches well with the Gaussian probability distribution function as can be seen in Figure 4.4.5. (a), because there is no fluctuation of the light intensity. When W=2 D (20 μm), the error between the light intensity and the fitting equation increases due to the fluctuation in light intensity, as shown in Figure 4.4.5. (b). Furthermore, the central peak of the fitting line is skewed from the center in the Height axis because the position of the breakup point for the PMMA suspension is not uniform, unlike the uniform localization of the Newtonian fluid. This is the effect of the added particles which appears when the filament becomes thin in the length scale of the particle diameter.

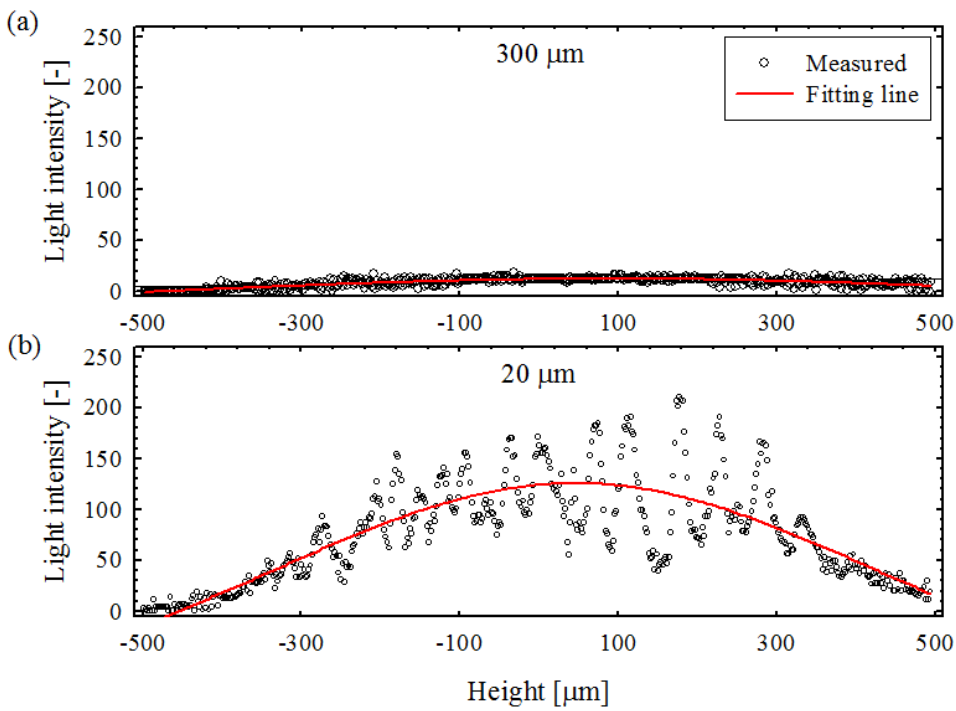

Figure 4.4.5. Measured light intensity of the 20 wt% PMMA suspension filament and fitting line using a 4 parameter Gaussian model at (a) *W*=300 μm, (b) *W*=20 μm. The numbers on the top of each graph are the minimum neck diameters.

Table 4.4.1. Fitting parameters in the Gaussian model at *W*=300 and 20 μm

Parameters	***W*=300 μm**	***W*=20 μm**
a	22.8	214.4
b	522.5	377.7
x_0	591.6	545.5
y_0	-15.9	-88.7

In order to analyze the randomness of the light intensity with the minimum neck diameter and particle concentration, the root-mean-square (ε_{rms}) of error (ε) between the fitting equation and the measured light intensity is calculated. The ε_{rms} describes the fluctuation of the light intensity. First, the ε_{rms} for pure silicone oil (Figure. 4.4.5 (a)), which is also used as the medium of the PMMA suspension, is as small as 5~10 μm, and is highly reproducible.

For the 20 wt% PMMA suspension, the change of ε_{rms} with the minimum neck diameter shows a different result. It begins to increase at W=20 D (200 μm) as seen in Figure 4.4.6 (b) because the fluctuation of the light intensity begins to increase as the minimum neck diameter decrease, as shown in Figure 4.4.5 (b). The important contribution in this graph is that the error bar of the ε_{rms} increases rapidly as the filament becomes thinner. The increase of the error bar is caused by random fluctuations in light intensity for W<10 D, as can be seen in Figure 4.4.4. In particular, the error bar increases rapidly at W=2 D, just before the pinch-off. The sudden increase of the heterogeneity is caused by the random distribution of the particles confined in the filament. The random particle distribution results in the random shape of the filament surface and the random pinch-off behavior.

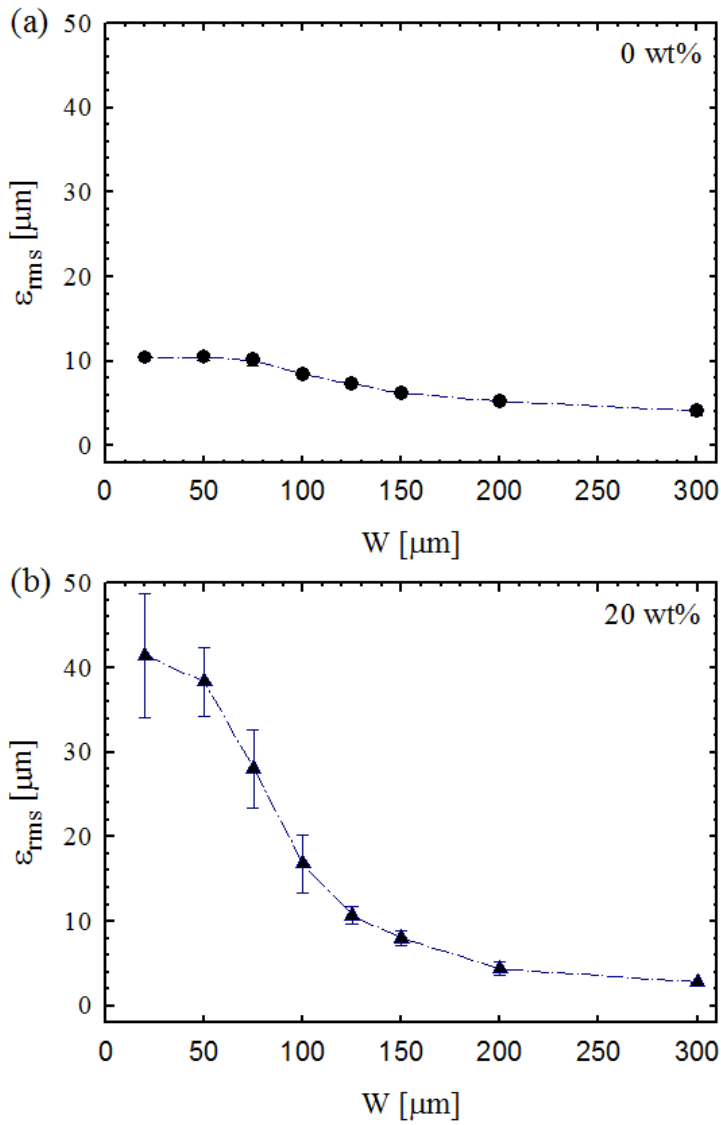

Figure 4.4.6. Root mean square error (ε_{rms}) of light intensity obtained by Gaussian model for (a) pure silicone oil of 0.40 Pa s and (b) the 20 wt% PMMA suspension depending on the minimum neck diameter (*W*). All the results were repeated three times.

Finally, Figure 4.4.7 shows the root mean square error of the light intensity depending on the particle concentration. For pure silicone oil (0 wt% in Figure 4.4.7), the ε_{rms} is low and the size of the error bar is very small even close to the pinch-off. However, the ε_{rms} and the size of the error bar increase rapidly with particle concentration. This means the confined particles increase the heterogeneity in the final stage of the filament breakup process as the particle concentration increases. The particles begin to affect the filament shape during the filament breakup as the filament becomes thinner than W=10 D (100 μm) and the particles induce the heterogeneity of the thinning filament under W=2 D (20 μm), which leads to the random pinch-off behavior. The heterogeneity is caused by the random distribution of the particles confined in the filament. We can conclude that the random and complex distribution of the particles plays a major role in developing the heterogeneous filament thinning process.

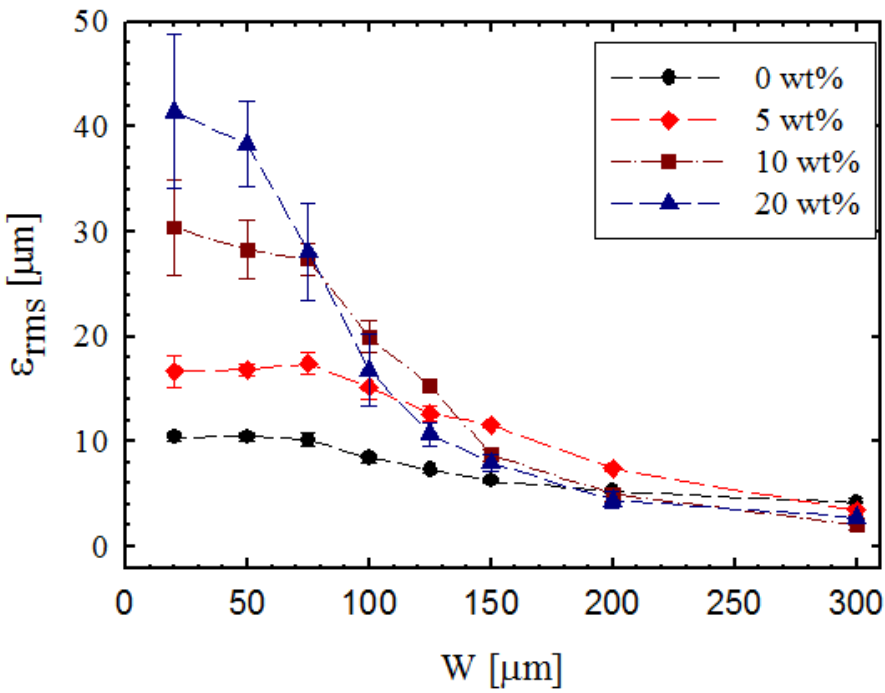

Figure 4.4.7. Root mean square of error (ε_{rms}) of the light intensity relative to the Gaussian probability distribution function for the pure silicone oil of 0.40 Pa s and the PMMA suspensions of 5, 10, 20 wt% PMMA particles.

Chapter 5.

Summary

The effect of the particles on the filament thinning under an extensional flow was investigated. The effect was more complicated in the final stages of the breakup process than in the initial stage. The particles induced significant changes in the breakup velocity, the filament shape, and the free surface roughness as the filament became thin in length scale of the particle diameter. A high-speed camera and high-resolution lens were used in order to visualize the process in the μm-length scale, in other words, to focus on the final stage of the filament thinning process.

The particles had different influences at various flow regimes. In the effective regime, i.e. in the initial stage of the breakup process, the particles increased the effective viscosity of the suspension and reduced the breakup velocity. The role of the particles was simple in this regime: when the filament of the PMMA suspension became thinner, the properties of the medium played a dominant role on the thinning dynamics. That is, the thinning dynamics appeared to be governed by the medium properties and were independent of the particle concentration. And the particles affected the process through decelerating the breakup process in this regime. However, as the filament approached the pinch-off ($0 < W < 5\ D$, W: minimum neck diameter, D: 10 μm, particle diameter), the particles induced instabilities resulting in the acceleration of the breakup velocity and increases in the roughness of the filament surface.

The particles did not affect the filament shape when the minimum neck diameter of the filament was larger than 10 D (100 μm). The filament shape of the PMMA suspension and of the Newtonian fluid having nearly identical viscosity and surface tension was the same in this regime ($W > 10\ D$). However, the particles began to

affect the filament shape when the filament became thinner than W=10 D. Then the particles induced a filament which had thick ends, but was still parabolic in shape like the Newtonian fluid. When the minimum neck diameter was reduced further down to 2 D (20 μm), the filament of the PMMA suspension became rough and random as it came close to the pinch-off. The particles induced non-uniformity in the filament breakup process as the minimum neck diameter of the filament became less than 2 D, that is, in the length scale of the particle diameter. The particles confined in the thinning filament were distributed randomly, and the particle concentration was locally non-uniform in the narrow filament. We observed that the particles were locally gathered or isolated when the filament became thinner than W=2 D. The distribution of the thick zones where the particles were present and the thin zones where the particles were absent was random, which led to a non-uniform filament thinning process. The random distribution of the particles caused heterogeneity in the filament shape, surface roughness, and pinch-off behavior.

In conclusion, the particles dispersed in a Newtonian fluid did not have an influence on the filament shape when the filament was thick, that is, larger than W=10 D. The particles began to produce an effect when the filament became thin, in the length scale of the particle diameter. As the filament became thinner than W=10 D, the shape of the filament was parabolic with thick ends, for 2 D<W<10 D. When the minimum neck diameter of the filament was reduced to less than 2 D, the particles induced a rough filament surface and random thinning behavior, and the heterogeneity was caused by the random distribution of the particles confined in the thinning filament.

Reference

Alexandrou, A. N., Bazilevskii, A. V., Entov, V. M., Rozhkov, A. N., and Sharaf, A. (2010). Breakup of a capillary bridge of suspensions. *Fluid Dyn*., 45(6), 952-964.

Amarouchene, Y., Bonn, D., Meunier, J., and Kellay, H. (2001). Inhibition of the finite-time singularity during droplet fission of a polymeric fluid. *Phys. Rev. Lett*., 86(16), 3558-3561.

Anna, S. L., and McKinley, G. H. (2001). Elasto-capillary thinning and breakup of model elastic liquids. *J. Rheol*., 45(1), 115-138.

Arnolds, O., Buggisch, H., Sachsenheimer, D., and Willenbacher, N. (2010). Capillary breakup extensional rheometry (CaBER) on semi-dilute and concentrated polyethyleneoxide (PEO) solutions. *Rheol. Acta*, 49(11), 1207-1217.

Basaran, O. A. (2002). Small-scale free surface flows with breakup: drop formation and emerging applications, *A .I. Ch. E. J*., 48(9), 1842-1848.

Basaran, O. A. (2010). Formation of beads-on-a-string structures during break-up of viscoelastic filaments. *Nat. Phys*., 6(8), 625-631.

Bender, J., and Wagner, N. J. (1996). Reversible shear thickening in monodisperse and bidisperse colloidal dispersions. *J. Rheol*., 40(5), 899-916.

Bertrand, T., Bonnoit, C., Clément, E., and Lindner, A. (2012). Dynamics of drop formation in granular suspensions: the role of volume fraction. *Granul. Matter*, 14(2), 169-174.

Bhat, P. P., Appathurai, S., Harris, M. T., Pasquali, M., McKinley, G. H., and

Bonnoit, C., Bertrand, T., Clément, E., and Lindner, A. (2012). Accelerated drop detachment in granular suspensions. *Phys. Fluids*, 24(4), 043304.

Bosse, T., Kleiser, L., Favre, J., and Meiburg, E. (2005). Settling and breakup of suspension drops. *Phys. Fluids*, 17(9), 091107.

Brenner, M. P., Shi, X. D., and Nagel, S. R. (1994). Iterated instabilities during droplet fission. *Phys. Rev. Lett.*, 73(25), 3391-3394.

Buttinoni, I., Bialké, J., Kümmel, F., Löwen, H., Bechinger, C., and Speck, T. (2013). Dynamical clustering and phase separation in suspensions of self-propelled colloidal particles. *Phys. Rev. Lett.*, 110(23), 238301.

Chang, H., and Demekhin, E. A. (1999). Iterated stretching of viscoelastic jets. *Phys. Fluids*, 11(7), 1717-1737.

Clasen, C., Eggers, J., Fontelos, M. A., Li, J., and McKinley, G. H. (2006). The beads-on-string structure of viscoelastic threads. *J. Fluid Mech*., 556, 283-308.

Day, R. F., Hinch, E. J., and Lister, J. R. (1998). Self-similar capillary pinchoff of an inviscid fluid. *Phys. Rev. Lett*., 80(4), 704-707.

DeGroot jr, J. V., Macosko, C. W., Kume, T., and Hashimoto, T. (1994). Flow-induced anisotropic SALS in silica-filled PDMS liquids. *J. Colloid Interf. Sci*., 166(2), 404-413.

Desse, M., Wolf, B., Mitchell, J., and Budtova, T. (2009). Experimental study of the break-up of starch suspension droplets in step-up shear flow. *J. Rheol*., 53(4), 943-955.

Dimic-Misic, K., Hummel, M., Paltakari, J., Sixta, H., Maloney, T., and Gane, P. (2015). From colloidal spheres to nanofibrils: Extensional flow properties

of mineral pigment and mixtures with micro and nanofibrils under progressive double layer suppression. *J. Colloid Interf. Sci*., 446, 31-43.

Eggers, J. (1993). Universal pinching of 3D axisymmetric free-surface flow. *Phys. Rev. Lett*., 71(21), 3458-3460.

Eggers, J. (1997). Nonlinear dynamics and breakup of free-surface flows. *Rev. Mod. Phys*., 69(3), 865-929.

Ehrl, L., Soos, M., and Morbidelli, M. (2008). Dependence of aggregate strength, structure, and light scattering properties on primary particle size under turbulent conditions in stirred-tank. *Langmuir*, 24(7), 3070-3081.

Entov, V. M., and Yarin, A. L. (1984). Influence of elastic stresses on the capillary breakup of dilute polymer solutions. *Fluid Dyn*., 19(1), 21-29.

Entov, V. M., and Hinch, E. J. (1997). Effect of a spectrum of relaxation times on the capillary thinning of a filament of elastic liquid. *J. Non-Newtonian Fluid Mech.*, 72(1), 31-54.

Fily, Y., and Marchetti, M. C. (2012). Athermal phase separation of self-propelled particles with no alignment. *Phys. Rev. Lett.*, 108(23), 235702.

Fontelos, M. A., and Li, J. (2004). On the evolution and rupture of filaments in Giesekus and FENE models. *J. Non-Newtonian Fluid Mech.*, 118(1), 1-16.

Furbank, R. J., and Morris, J. F. (2004). An experimental study of particle effects on drop formation. *Phys. Fluids*, 16(5), 1777-1790.

Furbank, R. J., and Morris, J. F. (2007). Pendant drop thread dynamics of particle-laden liquids. *Int. J. Multiphas. Flow*, 33(4), 448-468.

Gupta, V., Hampton, M. A., Stokes, J. R., Nguyen, A. V., and Miller, J. D. (2011). Particle interactions in kaolinite suspensions and corresponding aggregate

structures. *J. Colloid Interf. Sci*., 359(1), 95-103.

Hameed, M., and Morris, J. F. (2009). Breakup of a liquid jet containing solid particles: a singularity approach. *SIAM J. Appl. Math*., 70(3), 885-900.

Han, H., and Kim, C. (2015). Gelation of rod particle suspension in Newtonian fluid. *Korea Australia Rheol. J*., 27(2), 125-135.

James, D. F., McLean, B. D., and Saringer, J. H. (1987). Presheared extensional flow of dilute polymer solutions, *J. Rheol*., 31(6), 453-481.

Keller, J. B., and Miksis, M. J. (1983). Surface-tension driven flows. *SIAM J. Appl. Math.*, 43(2), 268-277.

Krieger, I. M., and Dougherty, T. J. (1959). A mechanism for non-Newtonian flow in suspensions of rigid spheres. *Trans. Soc. Rheol. (1957-1977)*, 3, 137-152.

Lee, M.-P., Hiltner, A., and Baer, E. (1992). Formation and break-up of a bead-and-string structure during injection moulding of a polycarbonate/acrylonitrile-butadiene-styrene blend. *Polymer*, 33(4), 675-684.

Li, J., and Fontelos, M. A. (2003). Drop dynamics on the beads-on-string structure for viscoelastic jets: a numerical study. *Phys. Fluids*, 15(4), 922-937.

Linse, P., and Lobaskin, V. (1999). Electrostatic attraction and phase separation in solutions of like-charged colloidal particles. *Phys. Rev. Lett*., 83(20), 4208-4311.

Lu, P. J., and Weitz, D. A. (2013). Colloidal particles: crystals, glasses, and gels. *Annu. Rev. Condens. Matter Phys*., 4(1), 217-233.

Manneville, S. (2008). Recent experimental probes of shear banding. *Rheol. Acta*, 47(3), 301-318.

Mathues, W., McIlroy, C., Harlen, O. G., and Clasen, C. (2015). Capillary breakup of suspensions near pinch-off. *Phys. Fluids*, 27(9), 093301.

McCready, E. M., and Burghardt, W. R. (2015). Structural response of a prealigned cylindrical block copolymer melt to extensional flow. *J. Rheol*., 59(4), 935-956.

McKinley, G. H., and Tripathi, A. (2000). How to extract the Newtonian viscosity from capillary breakup measurements in a filament rheometer. *J. Rheol*., 44(3), 653-670.

McKinley, G. H., and Sridhar, T. (2002). Filament-stretching rheometry of complex fluids. *Annu. Rev. Fluid Mech.*, 34, 375-415.

McKinley, G. H. (2005). Visco-elasto-capillary thinning and break-up of complex fluids. *Annu. Rheol. Rev.*, 1-48.

McIlroy, C., and Harlen, O. G. (2013). Modelling capillary break-up of particulate suspensions. *Phys. Fluids*, 26(3), 033101.

Montesi, A., Peña, A. A., and Pasquali, M. (2004). Vorticity alignment and negative normal stresses in sheared attractive emulsions. *Phys. Rev. Lett*., 92(5), 583031-583034.

Moon, J. Y., Lee, S. J., Ahn, K. H., and Lee, S. J. (2015). Filament thinning of silicone oil/PMMA suspensions under extensional flow. *Rheol. Acta*, 54(8), 705-714.

Moon, J. Y., Lee, S. J., Ahn, K. H., and Lee, S. J. (2015). Heterogeneity in the final stage of filament breakup of silicone oil/PMMA suspensions. *Rheol.*

Acta, Accepted (13 December 2015).

Mun, R. P., Byars, J. A., and Boger, D. V. (1998). The effects of polymer concentration and molecular weight on the breakup of laminar capillary jets. *J. Non-Newtonian Fluid Mech*., 74(1-3), 285-297.

Ogura, K., Morioka, K., Tsujii, Y., Hsu, S.-Y., and Wagner, M. H. (2015). Uniaxial extensional flow behavior of comb-shaped poly(methyl methacrylate). *Rheol. Acta*, 54(7), 637-645.

Oliveira, M. S. N., and McKinley, G. H. (2005). Iterated stretching and multiple beads-on-a-string phenomena in dilute solutions of highly extensible flexible polymers. *Phys. Fluids*, 17(7), 1-4.

Oliveira, M. S. N., Yeh, R., and McKinley, G. H. (2006). Iterated stretching, extensional rheology and formation of beads-on-a-string structures in polymer solutions. *J. Non-Newtonian Fluid Mech*., 137(1-3), 137-148.

Olmsted, P. D. (2008). Perspectives on shear banding in complex fluids. *Rheol. Acta*, 47(3), 283-300.

Ozel, B. G., Orum, A., Yildiz, M., and Menceloglu, Y. Z. (2014). Experimental study on the rheology of anisotropic, flocculated and low volume fraction colloids. *Korea Australia Rheol. J.*, 26(1), 105-116.

Papageorgiou, D. T. (1995). On the breakup of viscous liquid threads. *Phys. Fluids*, 7(7), 1529-1544.

Petrie, C. J. S. (1995). Extensional flow - a mathematical perspective, *Rheol. Acta*, 34(1), 12-26.

Plateau, J. (1843). *Acad. Sci. Bruxelles Me´m.*, 16, 34.

Plateau, J. (1849). *Acad. Sci. Bruxelles Me´m.*, 23, 5.

Rasmussen, H. K., and Hassager, O. (2001). The role of surface tension on the elastic decohesion of polymeric filaments. *J. Rheol*., 45(2), 527-537.

Rayleigh, J. W. S. (1892). On the instability of a cylinder if viscous liquid under capillary force. Phil. Mag. 34(207), 145-154.

Ren, Z., Harshe, Y. M., and Lattuada, M. (2015). Influence of the potential well on the breakage rate of colloidal aggregates in simple shear and uniaxial extensional flows. *Langmuir*, 31(21), 5712-5721.

Renardy, M. (1994). Some comments on the surface-tension driven breakup (or the lack of it) of viscoelastic jets. *J. Non-Newtonian Fluid Mech*., 51(1), 97-107.

Renardy, M. (2002). Similarity solutions for jet breakup for various models of viscoelastic fluids, *J. Non-Newtonian Fluid Mech.*, 104(1), 65-74.

Rodd, L. E., Scott, T. P., Cooper-White, J. J., and McKinley, G. H. (2005). Capillary break-up rheometry of low-viscosity elastic fluids. *Appl. Rheol.*, 15(1), 12-27.

Rothert, A., Richter, R., and Rehberg, I. (2003). Formation of a drop: viscosity dependence of three flow regimes. *N. J. Phys*., 5, 59.1-59.13.

Saha, D., Soos, M., Lüthi, B., Holzner, M., Liberzon, A., Babler, M.U., and Kinzelbach, W. (2014). Experimental characterization of breakage rate of colloidal aggregates in axisymmetric extensional flow. *Langmuir*, 30(48), 14385-14395.

Sattler, R., Gier, S., Eggers, J., and Wagner, C. (2012). The final stages of capillary break-up of polymer solutions. *Phys. Fluids*, 24(2), 023101.

So, J. H., Oh, W. K., and Yang, S. M. (2004). Microstructure and phase behavior

of concentrated silica particle suspensions. *Korean J. Chem. Eng*. 21(5), 921-928.

Spiegelberg, S. H., Gaudet, S., and McKinley, G. H. (1994). Extensional deformation of non-Newtonian materials: liquid bridge studies. *2nd Microgravity Fluid Physics Conference*. 3276, 311.

Stelter, M., Brenn, G., Yarin, A. L., Singh, R. P., and Durst, F. (2000). Validation and application of a novel elongational device for polymer solutions. *J. Rheol.*, 44(3), 595-616.

Stelter, M., Brenn, G., Yarin, A. L., Singh, R. P. and Durst, F. (2002). Investigation of the elongational behavior of polymer solutions by means of an elongational rheometer. *J. Rheol*., 46(2), 507-527.

Stokes, Y. M., Tuck, E. O., and Schwartz, L. W. (2000). Extensional fall of a very viscous drop. Q Jl. Mech. Appl. Math, 53(4), 565-582.

Tirtaatmadja, V., McKinley, G. H., and Cooper-White, J. J. (2006). Drop formation and breakup of low viscosity elastic fluids: effects of concentration and molecular weight. *Phys. Fluids*, 18(4), 043101.

van Deen, M. S., Bertrand, T., Vu, N., Quéré, D., Clément, E., and Lindner, A. (2013). Particles accelerate the detachment of viscous liquids. *Rheol. Acta*, 52(5), 403-412.

van Opheusden, J. H. J., and Molenaar, J. (2014). Phase segregation through transient network formation in a binary particle suspension in simple shear: application to dough. *Phys. Rev. E*. 89(4), 042305.

van Vliet, T., van Dijk, H. J. M., Zoon, P., and Walstra, P. (1991). Relation between syneresis and rheological properties of particle gels. *Colloid Polym.*

Sci., 269(6), 620-627.

Vermant, J., and Solomon, M. J. (2005). Flow-induced structure in colloidal suspensions. *J. Phys.: Condens. Matter*, 17(4), R187-R216.

Wagner, C., Amarouchene, Y., Bonn, D., and Eggers, J. (2005). Droplet detachment and satellite bead formation in viscoelastic fluids. *Phys. Rev. Lett.* 95(16), 164504.

Wagner, N. J., and Brady, J. F. (2009). Shear thickening in colloidal dispersions. *Phys. Today*, 62(10), 27-32.

White, E. E. B., Chellamuthu, M., and Rothstein, J. P. (2010). Extensional rheology of a shear-thickening cornstarch and water suspension. *Rheol. Acta*, 49(2), 119-129.

Wijmans, C. M., and Dickinson, E. (1998). Simulation of interfacial shear and dilatational rheology of an adsorbed protein monolayer modeled as a network of spherical particles. *Langmuir*, 14(25), 7278-7286.

Won, D., and Kim, C. (2004). Alignment and aggregation of spherical particles in viscoelastic fluid under shear flow. *J. Non-Newtonian Fluid Mech.*, 117(2-3), 141-146.

Xue, W., and Grest, G. S. (1990). Shear-induced alignment of colloidal particles in the presence of a shear flow. *Phys. Rev. Lett*., 64(4), 419-422.

Yanez, J. A., Shikata, T., Lange, F. F., and Pearson, D. S. (1996). Shear modulus and yield stress measurements of attractive alumina particle networks in aqueous slurries. *J. Am. Ceram. Soc*., 79(11), 2917-2924.

Zhao, H., Liu, H.-F., Xu, J.-L., Li, W.-F., and Lin, K.-F. (2015). Inhomogeneity in breakup of suspensions. *Phys. Fluids*, 27(6), 063303.

Zhang, X., Padgett, R. S., and Basaran, O. A. (1996). Nonlinear deformation and breakup of stretching liquid bridges. *J. Fluid Mech.*, 329, 207-245.

Zimoch, P. J., McKinley, G. H., and Hosoi, A. E. (2013). Capillary breakup of discontinuously rate thickening suspensions. *Phys. Rev. Lett.*, 111(3), 036001.

국문 초록

Silicone oil/PMMA 현탁액의 필라멘트 끊김 공정에 관한 연구

본 연구는 Newtonian 유체에 분산된 입자가 연신 흐름 하에서 현탁액의 필라멘트 끊김 공정에 미치는 영향에 대하여 논하였다. 특히, 끊김 공정의 마지막 단계에서 입자가 필라멘트에 미치는 영향에 대하여 집중적으로 살펴 보았는데, 이는 마지막 단계에서의 끊김 현상이 초기 단계의 그것보다 복잡하기 때문이다. 이와 같은 입자의 영향에 대해 연구하기 위하여, 10 μm 크기의 poly(methyl methacrylate) (PMMA) 입자 0~20 wt%를 silicone oil에 분산시켰다. PMMA 현탁액의 끊김 공정을 관찰함으로써 입자가 필라멘트의 최소 지름 (W) 에 따라 필라멘트의 끊김 역학과 모양에 미치는 영향에 대하여 연구 하였다.

첨가된 입자는 끊김 공정의 단계에 따라 서로 다른 역할을 하며 필라멘트의 끊김 역학에 영향을 미쳤다. 공정의 초기 단계에서 입자는 필라멘트의 최단 지름이 5 D (D=10 μm: 입자 지름)로 감소할 때까지는 끊김 속도를 감소 시켰고, 필라멘트가 W=5 D 이하로 가늘어져 완전히 끊어질 때까지는 끊김 속도를 급격하게 증가시켰다. 또한, 물성의 차이 없이 입자가 필라멘트의 끊김 공정에 미치는 영향에 대해 연구하기 위하여, PMMA 입자를 20 wt% 첨가한 PMMA 현탁액과 이와 점도,

표면장력의 크기를 맞춘 silicone oil의 끊김 속도를 비교하였다. 필라멘트의 최소 지름이 35 D 보다 클 때는, PMMA 현탁액과 물성의 크기를 맞춘 silicone oil의 시간 따른 필라멘트의 최소 지름의 변화 양상은 거의 일치하였다. 즉, 이 구간에서 필라멘트의 끊김 속도는 입자의 함량에 상관 없이 오직 유체의 점도와 표면장력의 크기에 의해 결정되었다. 하지만 필라멘트가 35 D 이하로 가늘어지면 두 필라멘트의 끊김 역학이 차이를 보이기 시작하는데, 첨가된 입자는 현탁액의 유효 점도를 증가시킬 뿐 아니라 PMMA 현탁액의 끊김 속도를 감소시켰다. 이는 필라멘트에 갇힌 입자가 연신 유동 하에서 유체의 흐름을 방해하기 때문이다.

앞의 20 wt% PMMA 현탁액과 이와 물성을 맞춘 silicone oil의 필라멘트 모양을 비교함으로써 입자가 필라멘트의 모양에 미치는 영향에 대해서 논하였다. 두 유체의 필라멘트가 W=10 D 보다 두꺼울 때, 두 유체의 필라멘트의 모양은 거의 같음을 관찰할 수 있었다. 이는 입자가 W>10 D의 구간에서는 필라멘트의 모양에 영향을 미치지 않음을 의미한다. 유체에 첨가된 입자는 필라멘트가 W=10 D 이하로 가늘어지면 필라멘트의 모양에 영향을 미치기 시작하였다. 필라멘트가 더욱 가늘어져 W<2 D 구간에서는 필라멘트의 표면이 거칠고 불균일 해지는 것을 확인할 수 있었고, 이는 필라멘트가 임의로 끊어지는 현상으로 이어졌다. 이러한 불균임함은 필라멘트가 입자 지름의 길이 단위로 가늘어졌을 때, 필라멘트 내부에 갇힌 입자들의 국부적인 농도 차이에

의해 유발되었다. 이와 같은 입자들의 불균일한 분포가 필라멘트 끊김 공정의 마지막 단계에서 관찰되는 불균일한 끊김 공정을 유발하는 것을 확인할 수 있었다. 입자의 불균일한 분포는 가늘어지는 필라멘트 중심부의 밝기 분석을 통하여 정량화 되었다.

이처럼 유체에 첨가된 입자가 필라멘트 끊김 공정에 미치는 영향은 초기 단계에서 보다 마지막 단계에서 복잡하고 불균일한 양상을 띄었고, 마지막 단계에서의 복잡성과 불균일성에 대하여 논하였다. 본 연구는 입자가 현탁액의 필라멘트 끊김 공정에서 필라멘트의 끊김 역학과 모양에 미치는 영향에 대한 정보를 제공하고 있고, 입자가 필라멘트 끊김 공정에 미치는 영향에 대한 정보들은 코팅, 젯팅, 스프레잉 같은 연신 흐름 공정을 설계하는데 있어 대단히 유용한 역할을 할 것이라 기대한다.

주요어: 유동 가시화, 필라멘트 끊김, silicone oil/PMMA 현탁액, 임의의 끊김 현상, 임의의 입자 분포

학번: 2008-22980